Supporting Information

Supplementary Materials: Figure S1: Schematic illustration of the typical mechanisms of nucleation and growth of ionic liquid films; Figure S2: Schematic representation of the vacuum thermal evaporation methodology; Figure S3: Schematic representation of the ovens of the ThinFilmVD apparatus and an image of an individual oven; Figure S4: Schematic representation and images of the substrates support system; Figure S5: Morphology of the substrates (ITO/glass and Ag/ITO/glass); Figures S6-S17: Morphology of [C_2C_1im][NTf_2] (S6), [C_2C_1im][OTf] (S9), [C_8C_1im][NTf_2] (S12), and [C_2C_1im][OTf] (S15) films on ITO and Ag using Knudsen effusion cells with different orifice diameters and employing different evaporation temperatures and the respective size distribution of the droplets (S7, S8, S10, S11, S13, S14, S16, and S17). Figure S18-S21: Morphology of micro-/nanodroplets of [C_2C_1im][NTf_2] (S18), [C_2C_1im][OTf] (S19), [C_8C_1im][NTf_2] (S20), and [C_2C_1im][OTf] (S21) fabricated onto ITO/glass and Ag/ITO/glass using Knudsen effusion cells with different orifice diameters; Figure S22-S29: Morphology of micro-/nanodroplets of [C_2C_1im][NTf_2] (S22), [C_2C_1im][OTf] (S24), [C_8C_1im][NTf_2] (S26), and [C_2C_1im][OTf] (S28) fabricated onto ITO/glass and Ag/ITO/glass employing different substrate temperatures and the respective size distribution (S23, S25, S27, and S29); Table S1: Experimental conditions related to the study of the effect of the mass flow rate on the morphology of the ionic liquid films deposited on ITO/glass and Ag/ITO/glass surfaces; Table S2: Experimental conditions related to the study of the effect of the substrate temperature on the morphology of the ionic liquid films deposited on ITO/glass and Ag/ITO/glass surfaces.

Index

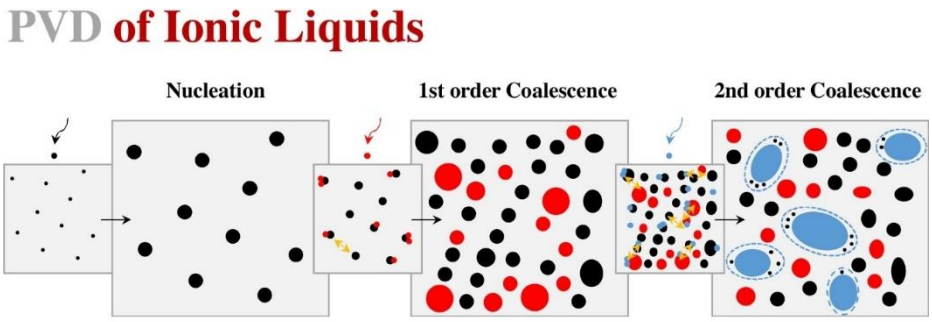

Figure S1. Schematic illustration of the typical mechanisms of nucleation and growth of ionic liquid films obtained by vapor deposition: minimum free area to promote nucleation (MFAN); first-order coalescence; second-order coalescence. More details: *Appl. Surf. Sci.*, 2018, 428, 242.

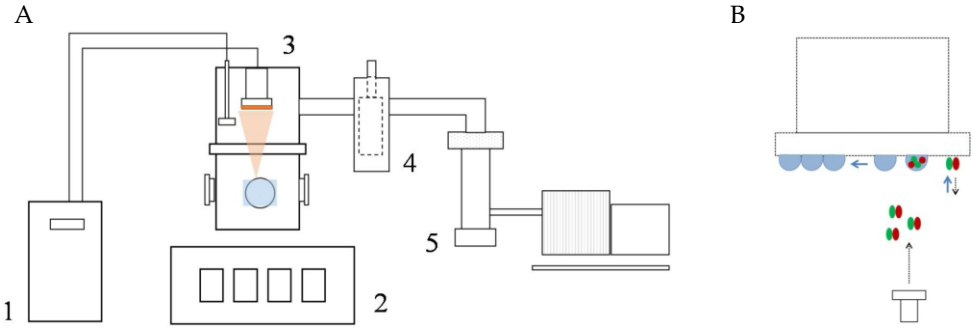

Figure S2. Schematic representation of the vacuum thermal evaporation methodology: (A) ThinFilmVD apparatus (1 – cooling system, 2 – instrumentation box, 3 – vacuum chamber, 4 – N_2 (l) metallic trap, 5 – vacuum pumping system); (B) schematic detail of the PVD of ionic liquids by thermal evaporation from a Knudsen cell. More details: *Appl. Surf. Sci.*, 2018, 428, 242 and *J. Chem. Eng. Data*, 2015, 60, 3776.

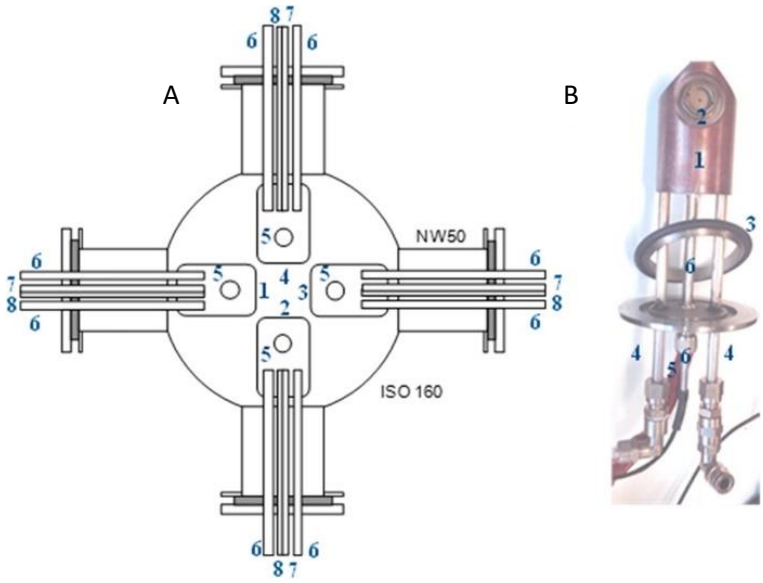

Figure S3. A – Schematic representation of the ovens of the ThinFilmVD apparatus: 1, 2, 3, 4 – individual copper ovens; 5 – cavity of the Knudsen cell screwing; 6 – air cooling tube; 7 – heater; 8, – Pt100 sensor; B – Image of an individual oven (top view): 1 – copper block; 2 – Knudsen cell; 3 – Viton O-ring; 4 – cooling system; 5 – heater; 6 – Pt100. More details: *J. Chem. Eng. Data*, 2015, 60, 3776.

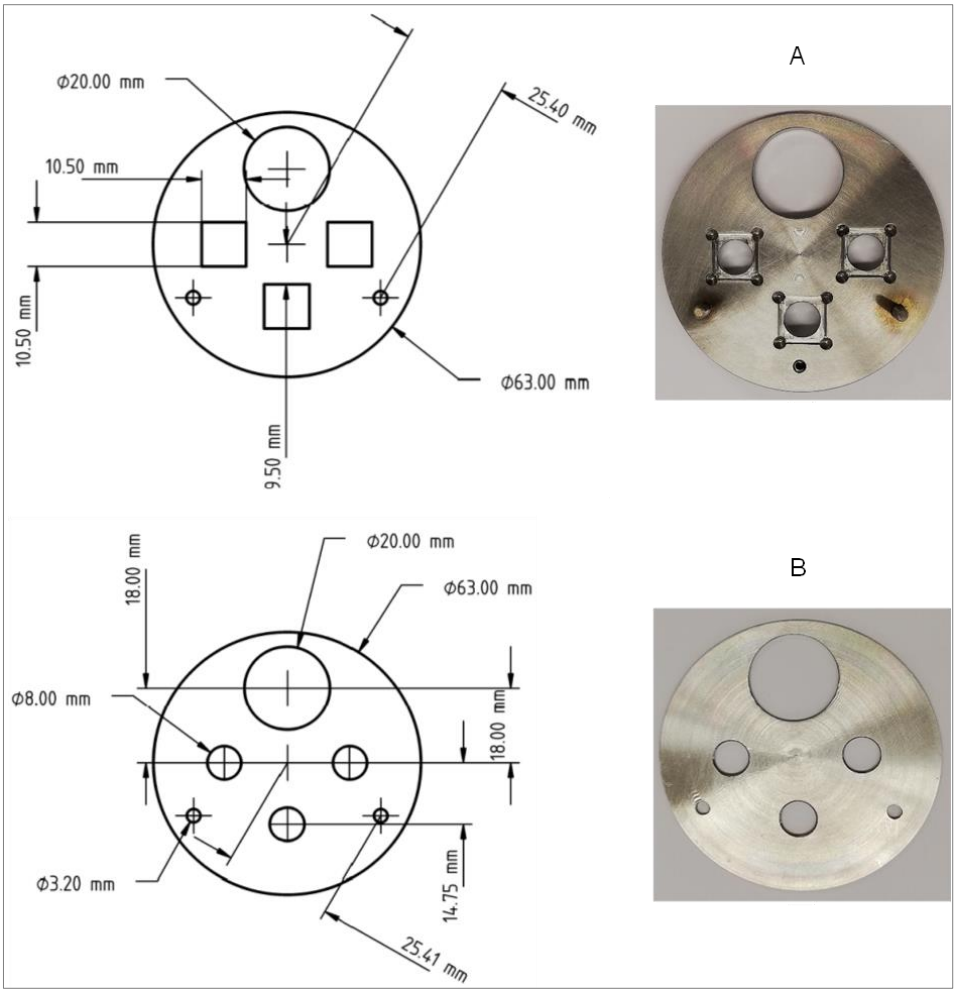

Figure S4. Schematic representation (left) and images (right) of the substrate support system. The support was used for the simultaneous deposition of each ionic liquid on different surfaces: ITO/glass; Ag/ITO/glass.

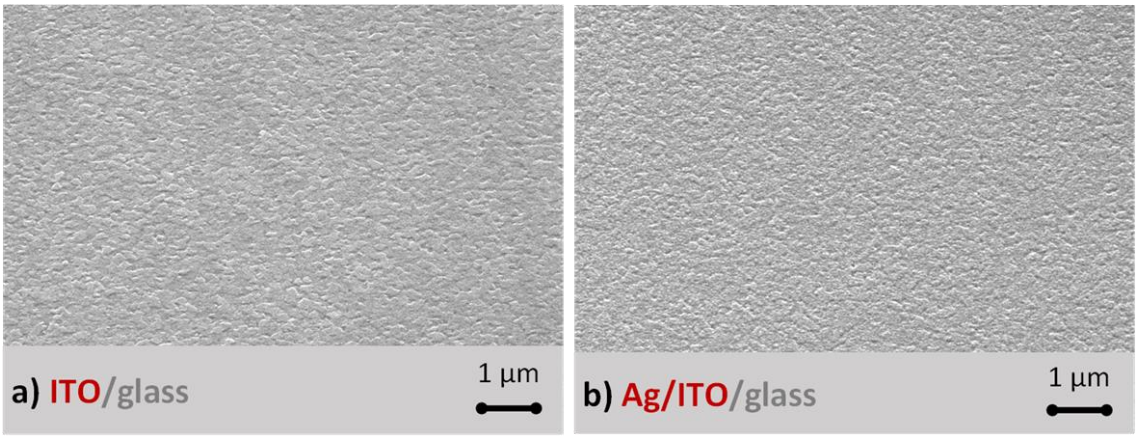

Figure S5. Morphology of the substrates: indium tin oxide (ITO)/glass surface (a); silver (Ag)/ITO/glass surface (b). Micrographs were acquired through high-resolution scanning electron microscopy (SEM) by using a secondary electron detector (SED). Lateral views at 45° were obtained with a magnification of 25000×.

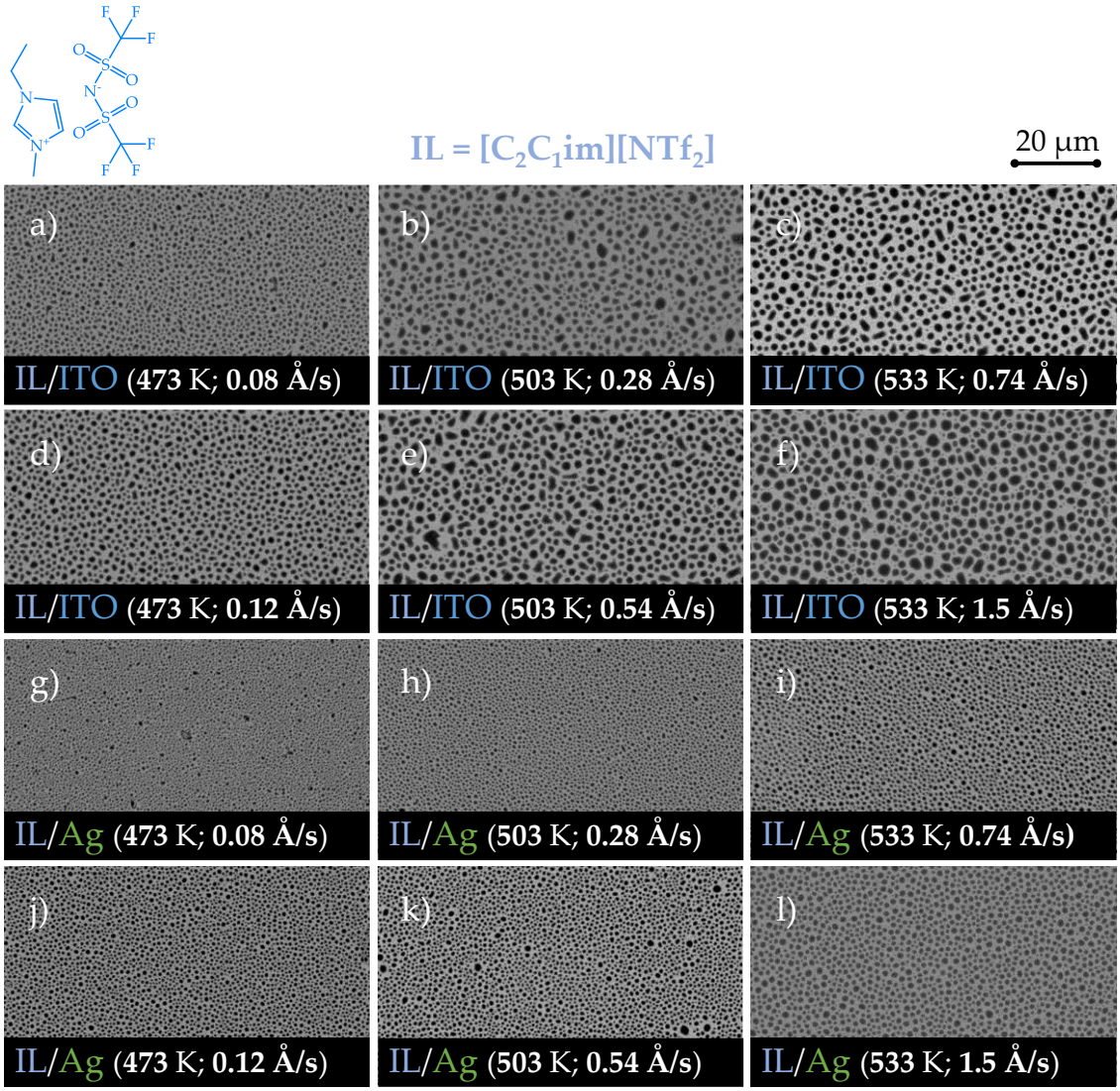

Figure S6. Morphology of micro-/nanodroplets of [C_2C_1im][NTf_2] (40 ML) fabricated by vacuum thermal evaporation onto ITO/glass (a, b, c, d, e, f) and Ag/ITO/glass (g, h, i, j, k, l) using Knudsen effusion cells with different orifice diameters (2 or 3 mm) and employing different evaporation temperatures (473, 503, or 533 K): 2 mm, 473 K (a, g); 3 mm, 473 K (d, j); 2 mm, 503 K (b, h); 3 mm, 503 K (e, k); 2 mm, 533 K (c, i); 3 mm, 533 K (f, l). The average surface coverage (SC) of the microdroplets was derived by image processing of the SEM micrographs (images a to l): SC of (34.1 ± 3.6) % and SC of (34.0 ± 1.3) % were obtained for IL films deposited onto surfaces of ITO and Ag, respectively. The substrate temperature was kept at 283 K. SEM micrographs (top views) were obtained by backscattered electron imaging.

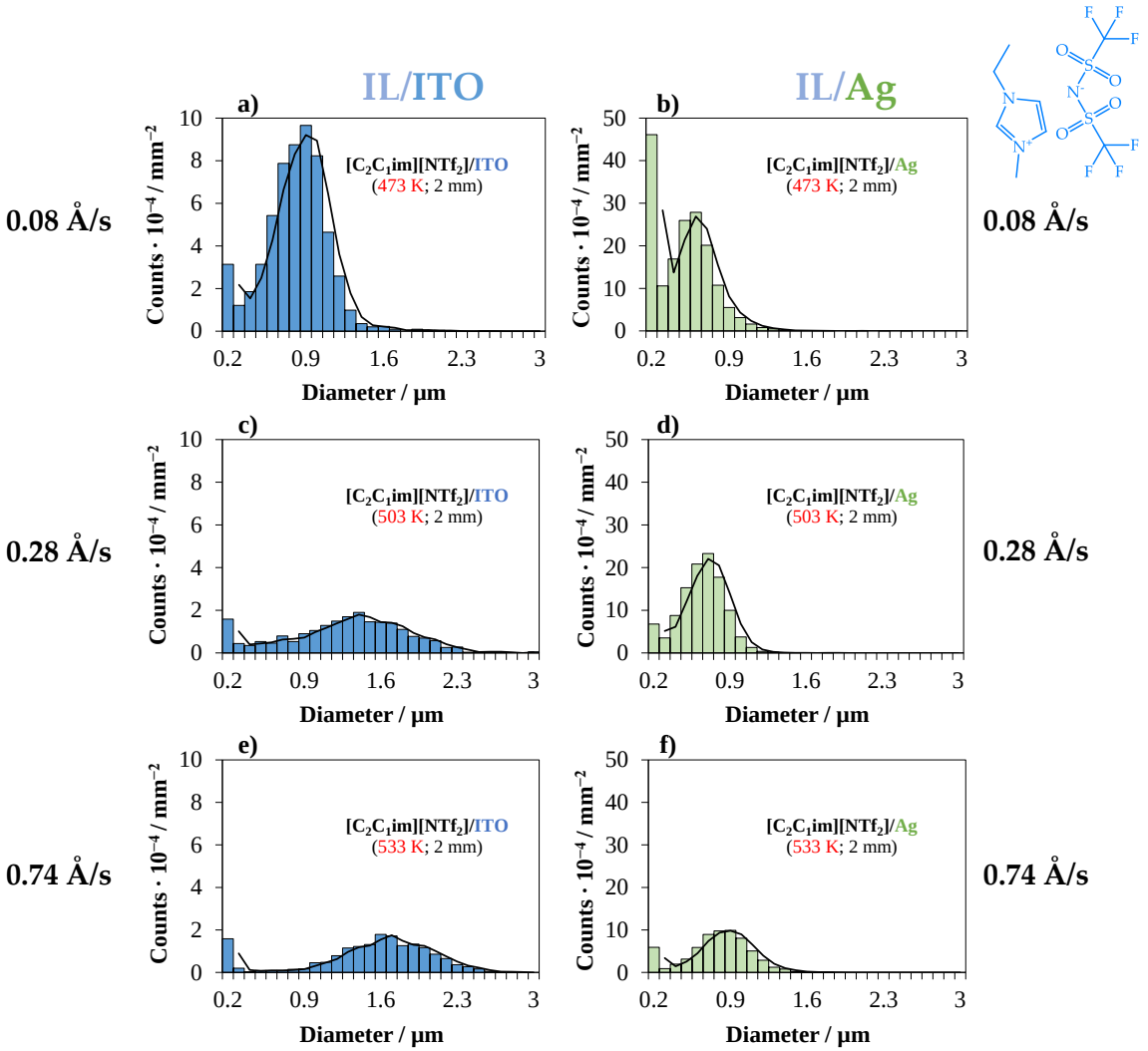

Figure S7. Size distribution of micro-/nanodroplets of [C2C1im][NTf2] (40 ML) fabricated by vacuum thermal evaporation onto ITO/glass (a, c, e) and Ag/ITO/glass (b, d, f) using a Knudsen effusion cell (orifice diameter of 2 mm) and employing different evaporation temperatures/different deposition rates: 473 K (a, b); 503 K (c, d); 533 K (e, f). The substrate temperature was kept at 283 K.

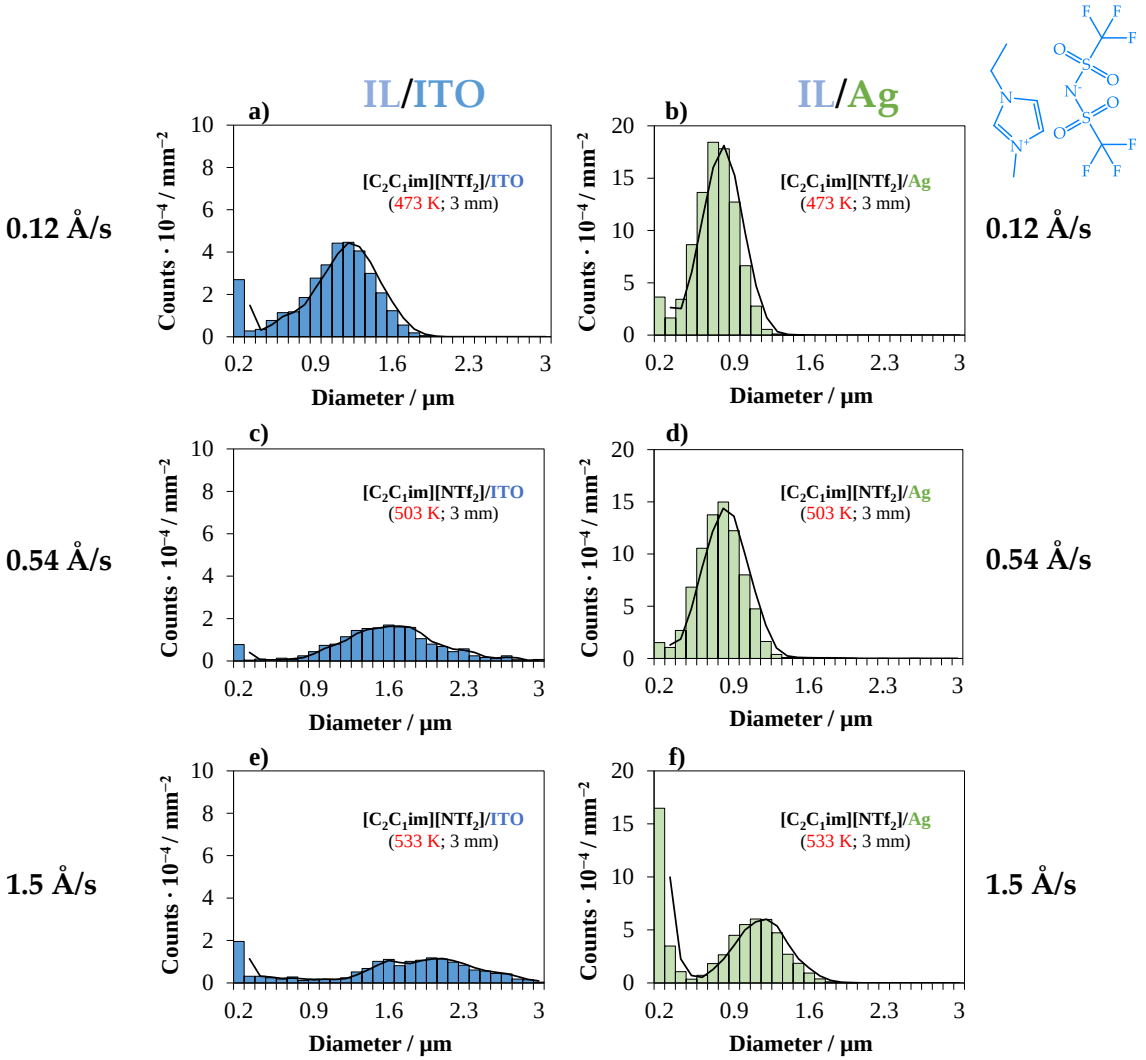

Figure S8. Size distribution of micro-/nanodroplets of [C2C1im][NTf2] (40 ML) fabricated by vacuum thermal evaporation onto ITO/glass (a, c, e) and Ag/ITO/glass (b, d, f) using a Knudsen effusion cell (orifice diameter of 3 mm) and employing different evaporation temperatures/different deposition rates: 473 K (a, b); 503 K (c, d); 533 K (e, f). The substrate temperature was kept at 283 K.

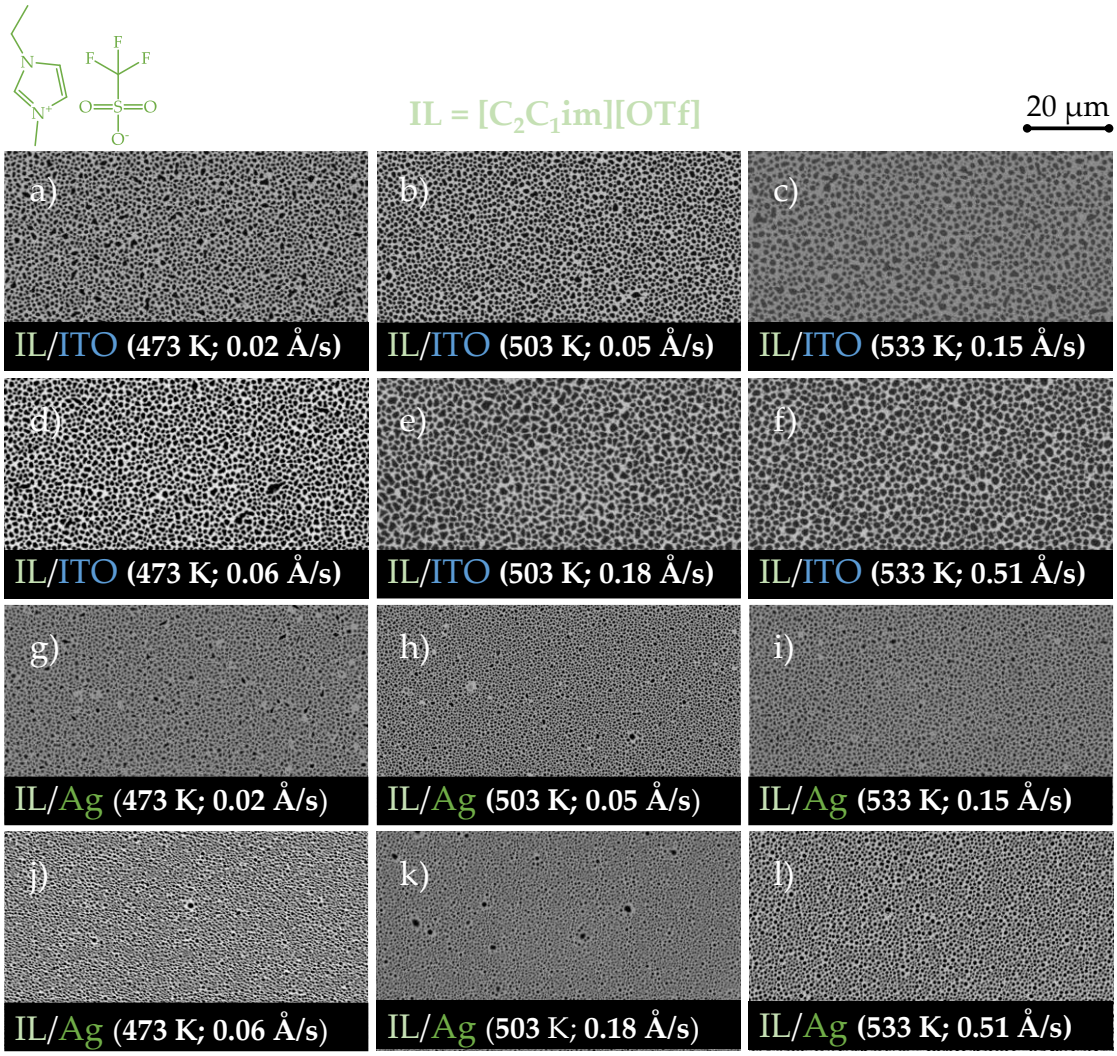

Figure S9. Morphology of micro-/nanodroplets of [C_2C_1im][OTf] (40 ML) fabricated by vacuum thermal evaporation onto ITO/glass (a, b, c, d, e, f) and Ag/ITO/glass (g, h, i, j, k, l) using Knudsen effusion cells with different orifice diameters (2 or 3 mm) and employing different evaporation temperatures (473, 503, or 533 K): 2 mm, 473 K (a, g); 3 mm, 473 K (d, j); 2 mm, 503 K (b, h); 3 mm, 503 K (e, k); 2 mm, 533 K (c, i); 3 mm, 533 K (f, l). The average surface coverage (SC) of the microdroplets was derived by image processing of the SEM micrographs (images a to l): SC of (43.9 ± 3.6) % and SC of (38.9 ± 1.6) % were obtained for IL films deposited onto surfaces of ITO and Ag, respectively. The substrate temperature was kept at 283 K. SEM micrographs (top views) were obtained by backscattered electron imaging.

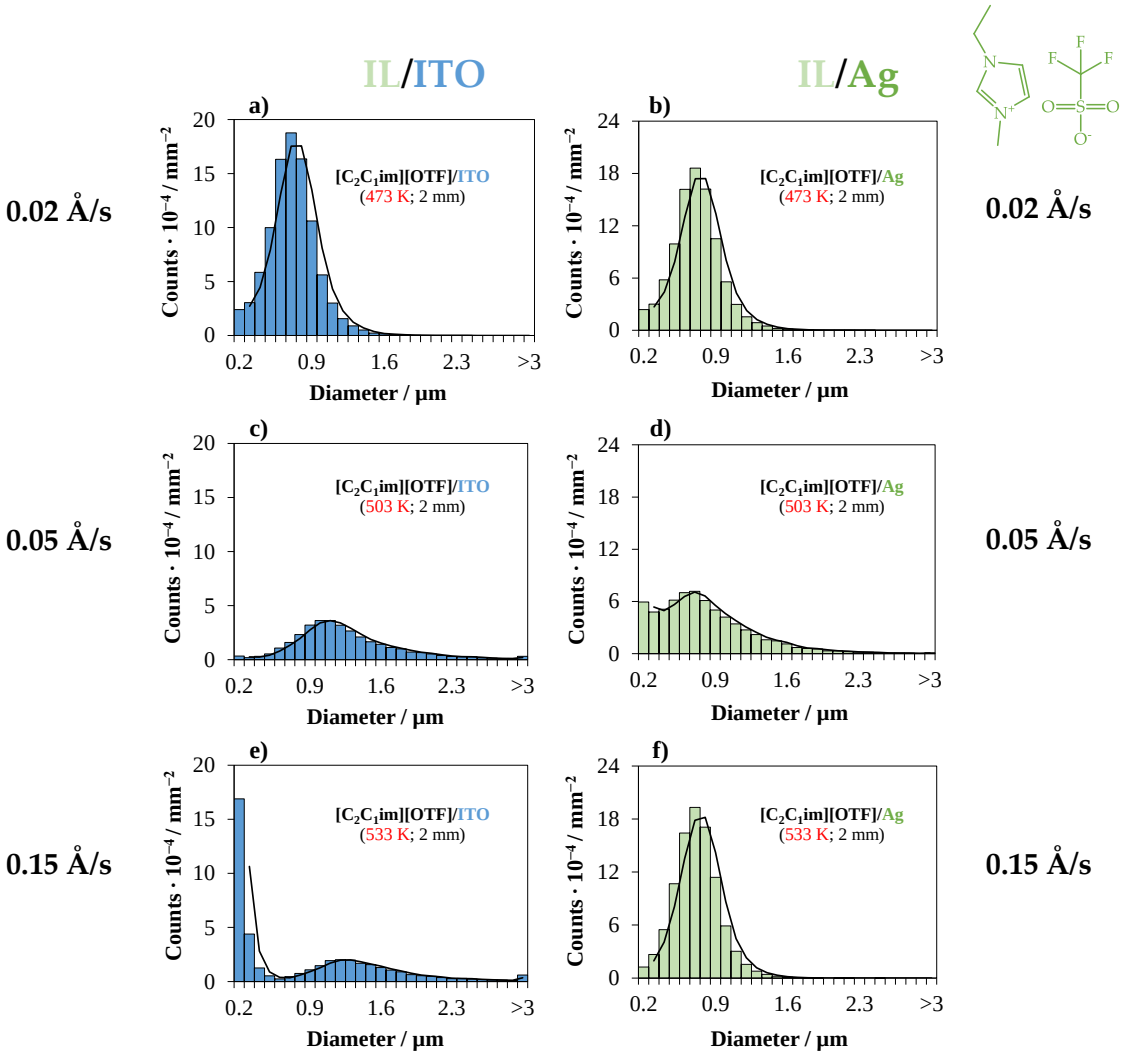

Figure S10. Size distribution of micro-/nanodroplets of [C2C1im][OTf] (40 ML) fabricated by vacuum thermal evaporation onto ITO/glass (a, c, e) and Ag/ITO/glass (b, d, f) using a Knudsen effusion cell (orifice diameter of 2 mm) and employing different evaporation temperatures/different deposition rates: 473 K (a, b); 503 K (c, d); 533 K (e, f). The substrate temperature was kept at 283 K.

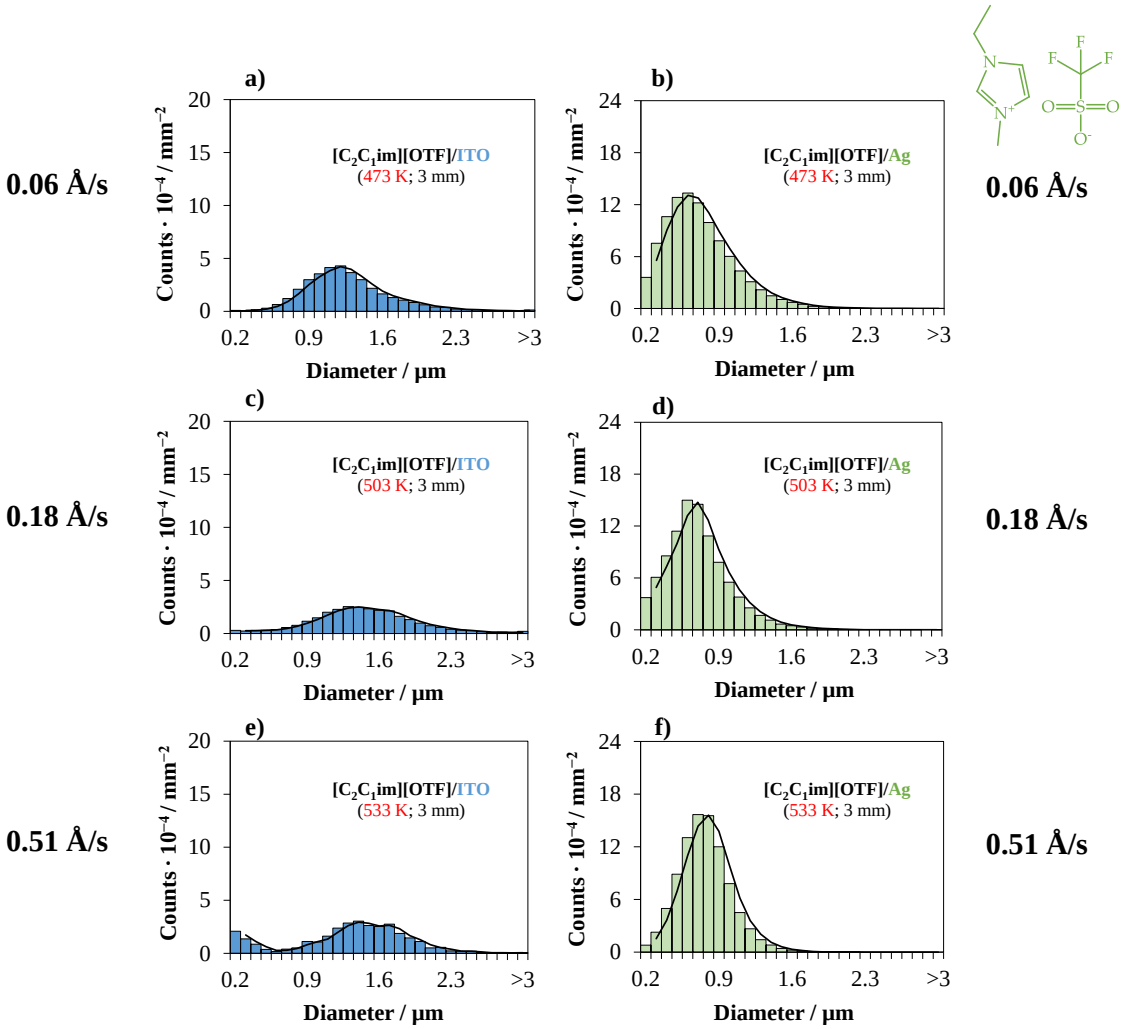

Figure S11. Size distribution of micro-/nanodroplets of [C2C1im][OTf] (40 ML) fabricated by vacuum thermal evaporation onto ITO/glass (a, c, e) and Ag/ITO/glass (b, d, f) using a Knudsen effusion cell (orifice diameter of 3 mm) and employing different evaporation temperatures/different deposition rates: 473 K (a, b); 503 K (c, d); 533 K (e, f). The substrate temperature was kept at 283 K.

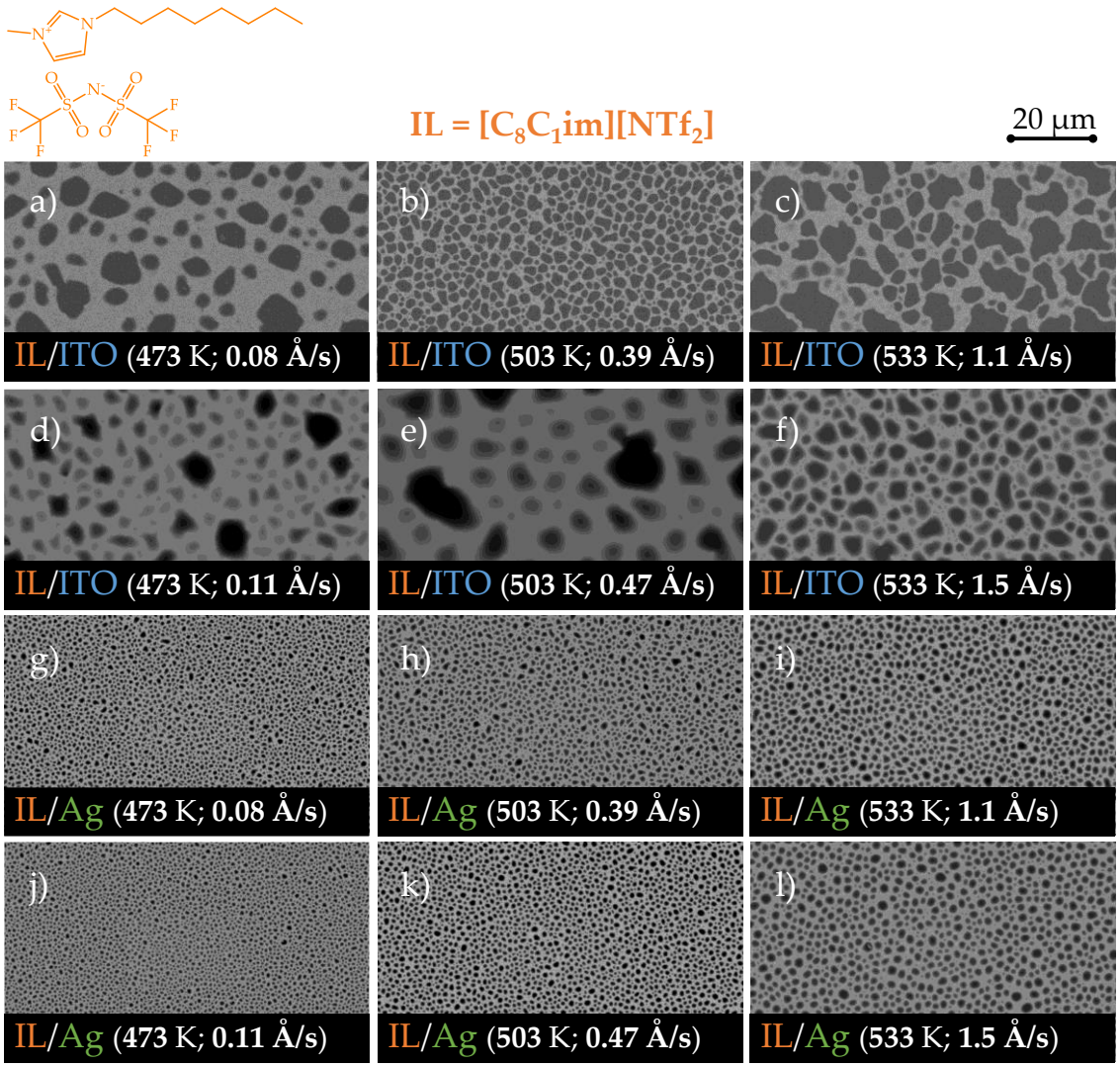

Figure S12. Morphology of micro-/nanodroplets of [C_8C_1im][NTf_2] (40 ML) fabricated by vacuum thermal evaporation onto ITO/glass (a, b, c, d, e, f) and Ag/ITO/glass (g, h, i, j, k, l) using Knudsen effusion cells with different orifice diameters (2 or 3 mm) and employing different evaporation temperatures (473, 503, or 533 K): 2 mm, 473 K (a, g); 3 mm, 473 K (d, j); 2 mm, 503 K (b, h); 3 mm, 503 K (e, k); 2 mm, 533 K (c, i); 3 mm, 533 K (f, l). The image processing was not able to derive with accuracy the surface coverage of the films (it is estimated to be higher than 40 %). The substrate temperature was kept at 283 K. SEM micrographs (top views) were obtained by backscattered electron imaging.

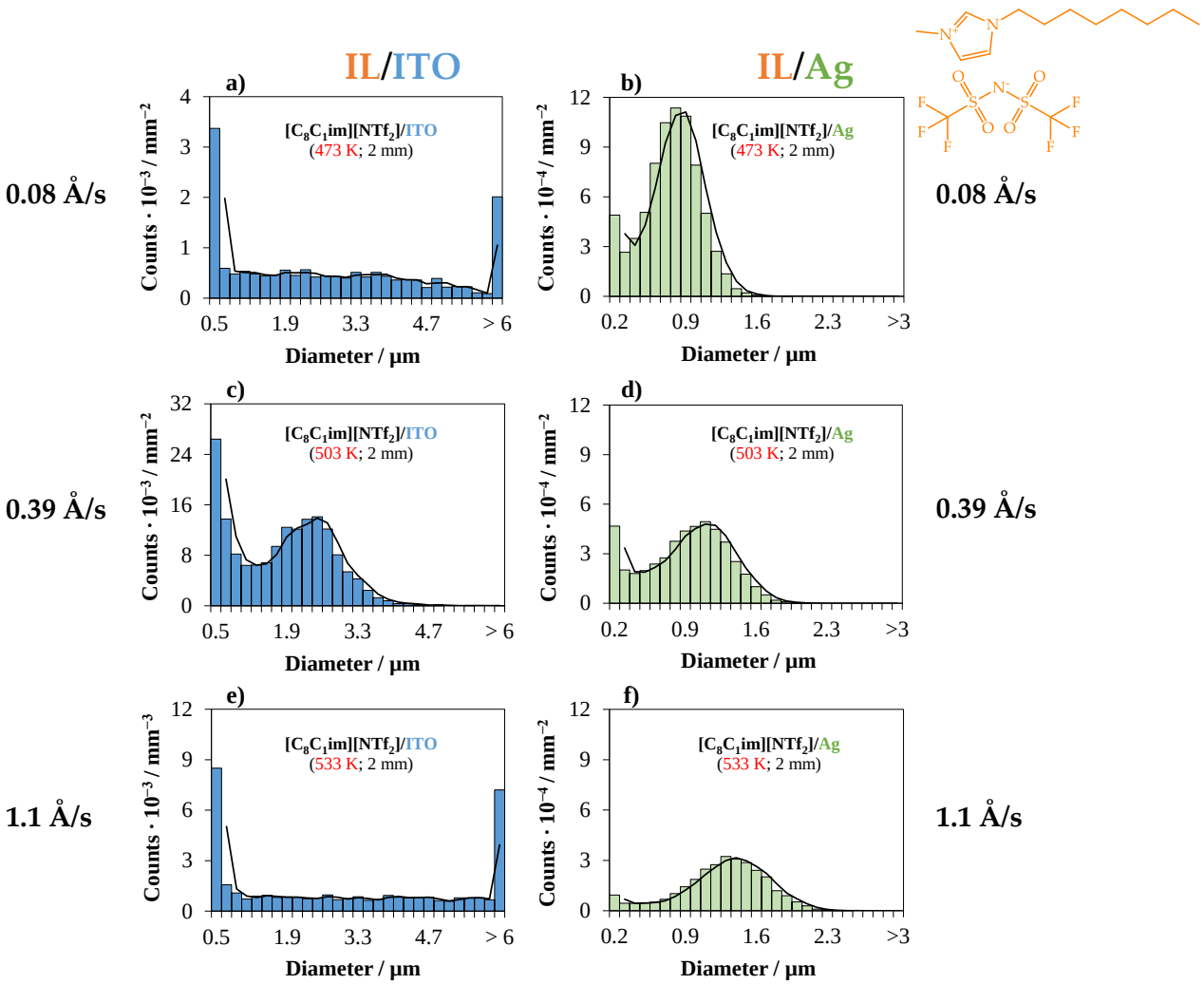

Figure S13. Size distribution of micro-/nanodroplets of [C8C1im][NTf2] (40 ML) fabricated by vacuum thermal evaporation onto ITO/glass (a, c, e) and Ag/ITO/glass (b, d, f) using a Knudsen effusion cell (orifice diameter of 2 mm) and employing different evaporation temperatures/different deposition rates: 473 K (a, b); 503 K (c, d); 533 K (e, f). The substrate temperature was kept at 283 K.

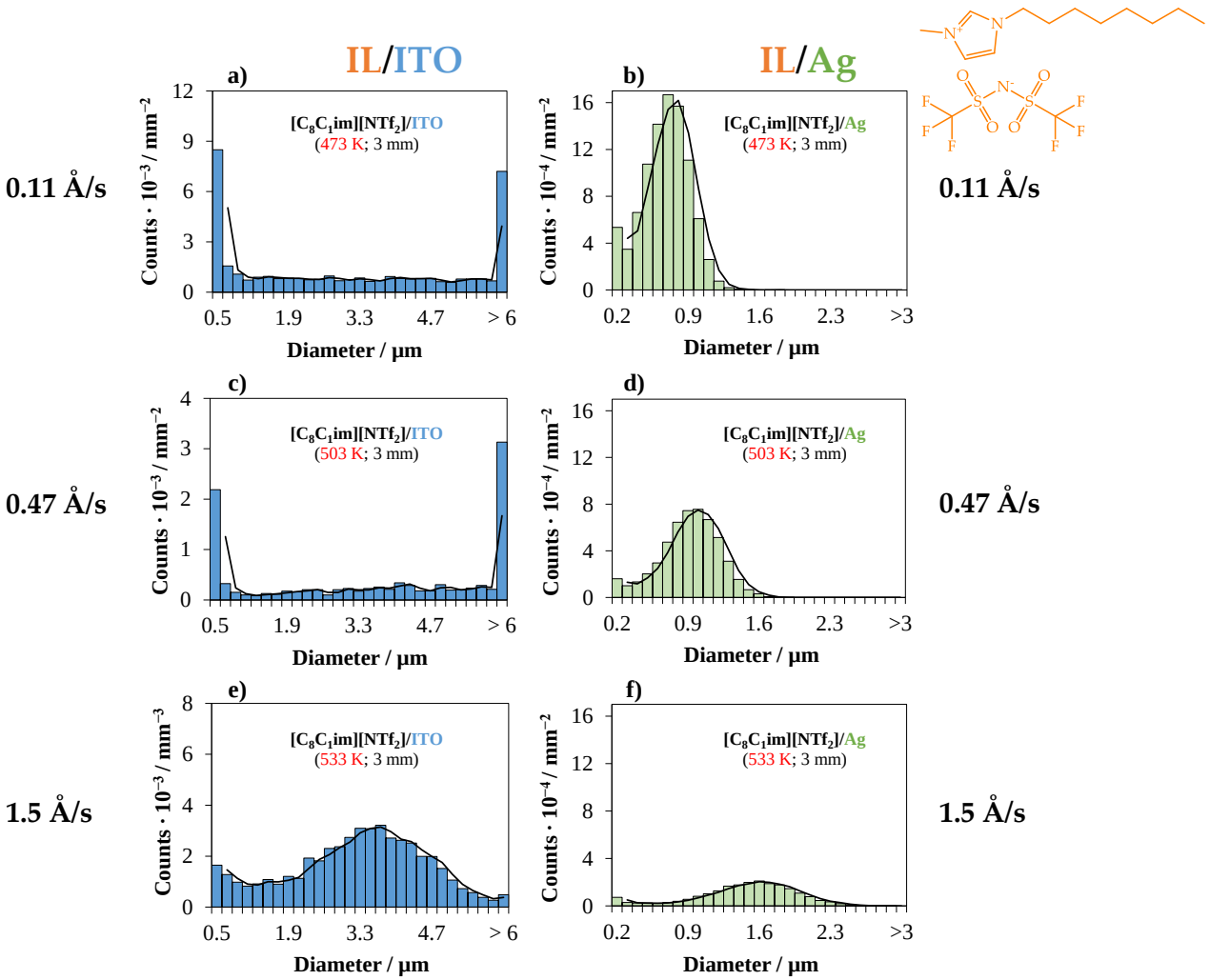

Figure S14. Size distribution of micro-/nanodroplets of [C8C1im][NTf2] (40 ML) fabricated by vacuum thermal evaporation onto ITO/glass (a, c, e) and Ag/ITO/glass (b, d, f) using a Knudsen effusion cell (orifice diameter of 3 mm) and employing different evaporation temperatures/different deposition rates: 473 K (a, b); 503 K (c, d); 533 K (e, f). The substrate temperature was kept at 283 K.

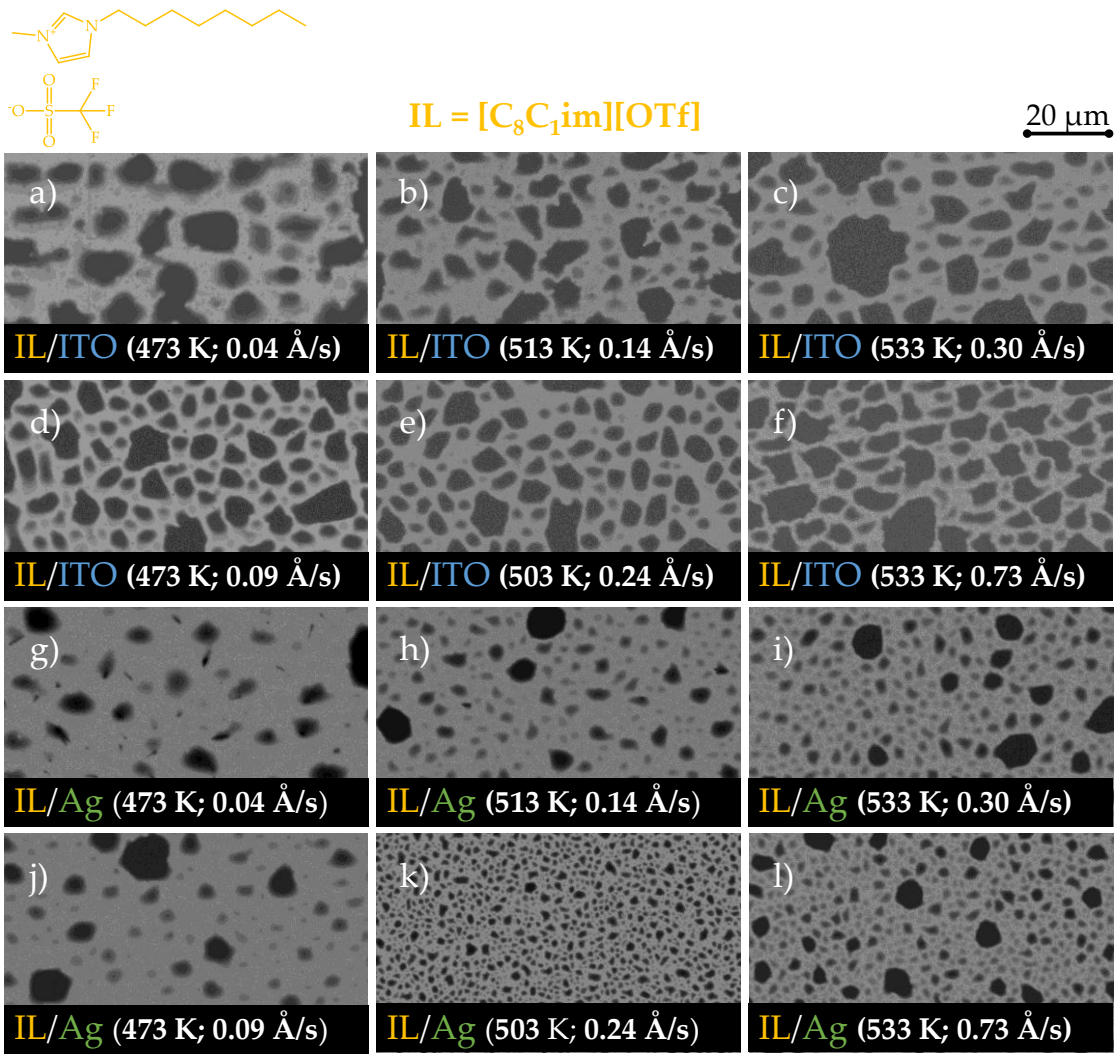

Figure S15. Morphology of micro-/nanodroplets of [C8C1im][OTf] (40 ML) fabricated by vacuum thermal evaporation onto ITO/glass (a, b, c, d, e, f) and Ag/ITO/glass (g, h, i, j, k, l) using Knudsen effusion cells with different orifice diameters (2 or 3 mm) and employing different evaporation temperatures (473, 503, 513 or 533 K): 2 mm, 473 K (a, g); 3 mm, 473 K (d, j); 2 mm, 513 K (b, h); 3 mm, 503 K (e, k); 2 mm, 533 K (c, i); 3 mm, 533 K (f, l). The image processing was not able to derive with accuracy the surface coverage of the films (it is estimated to be higher than 40 %). The substrate temperature was kept at 283 K. SEM micrographs (top views) were obtained by backscattered electron imaging.

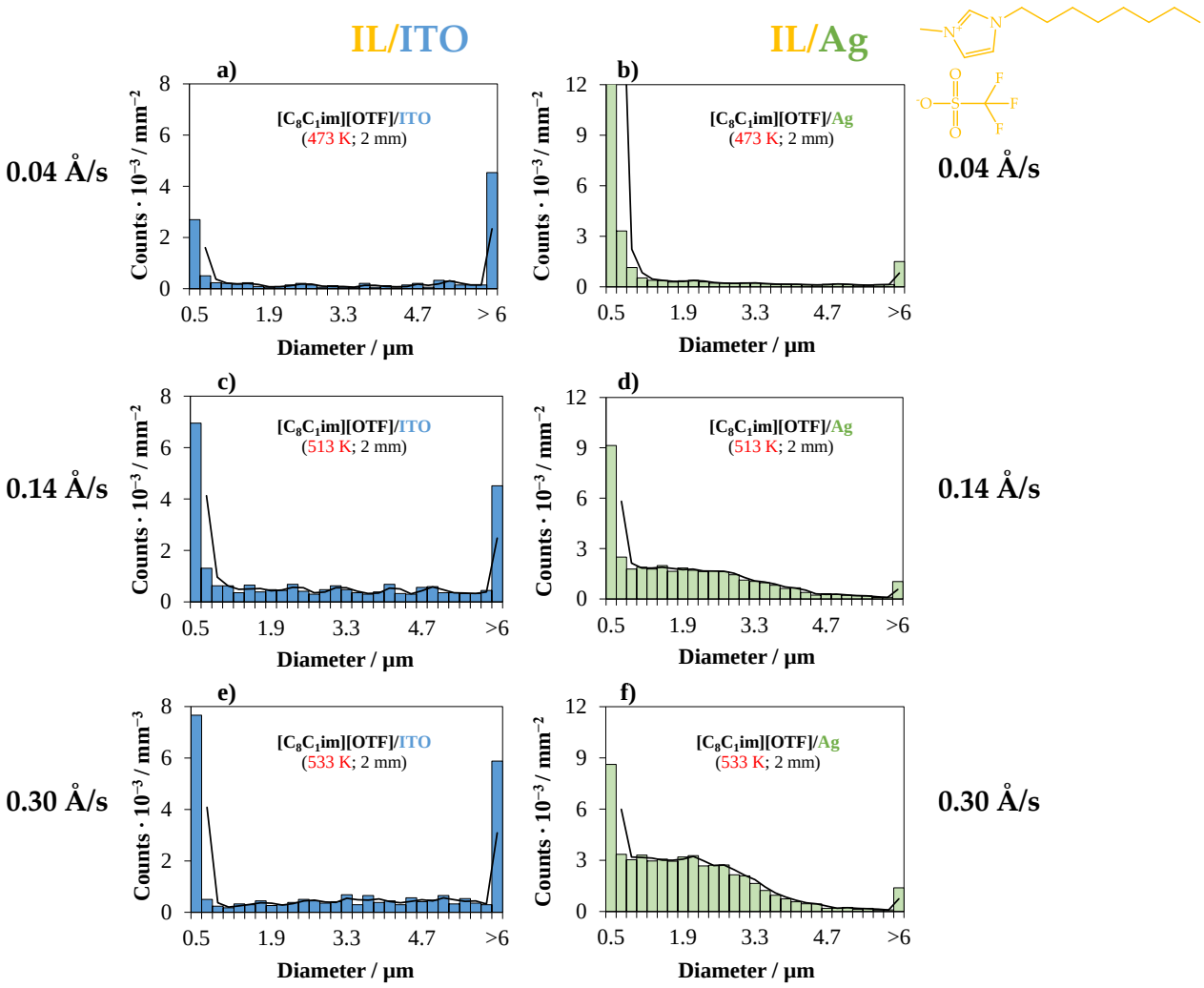

Figure S16. Size distribution of micro-/nanodroplets of [C8C1im][OTf] (40 ML) fabricated by vacuum thermal evaporation onto ITO/glass (a, c, e) and Ag/ITO/glass (b, d, f) using a Knudsen effusion cell (orifice diameter of 2 mm) and employing different evaporation temperatures/different deposition rates: 473 K (a, b); 513 K (c, d); 533 K (e, f). The substrate temperature was kept at 283 K.

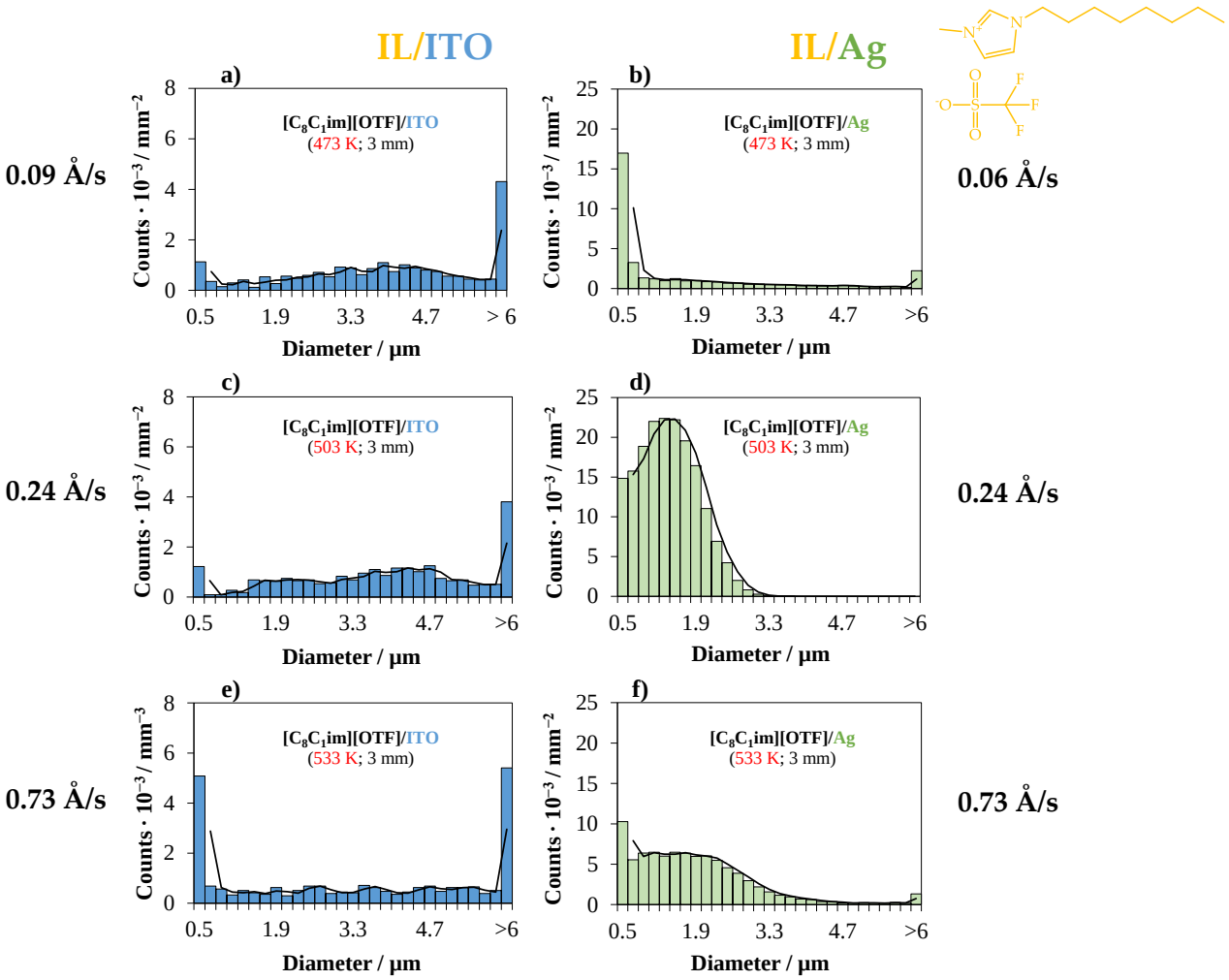

Figure S17. Size distribution of micro-/nanodroplets of [C8C1im][OTf] (40 ML) fabricated by vacuum thermal evaporation onto ITO/glass (a, c, e) and Ag/ITO/glass (b, d, f) using a Knudsen effusion cell (orifice diameter of 3 mm) and employing different evaporation temperatures/different deposition rates: 473 K (a, b); 503 K (c, d); 533 K (e, f). The substrate temperature was kept at 283 K.

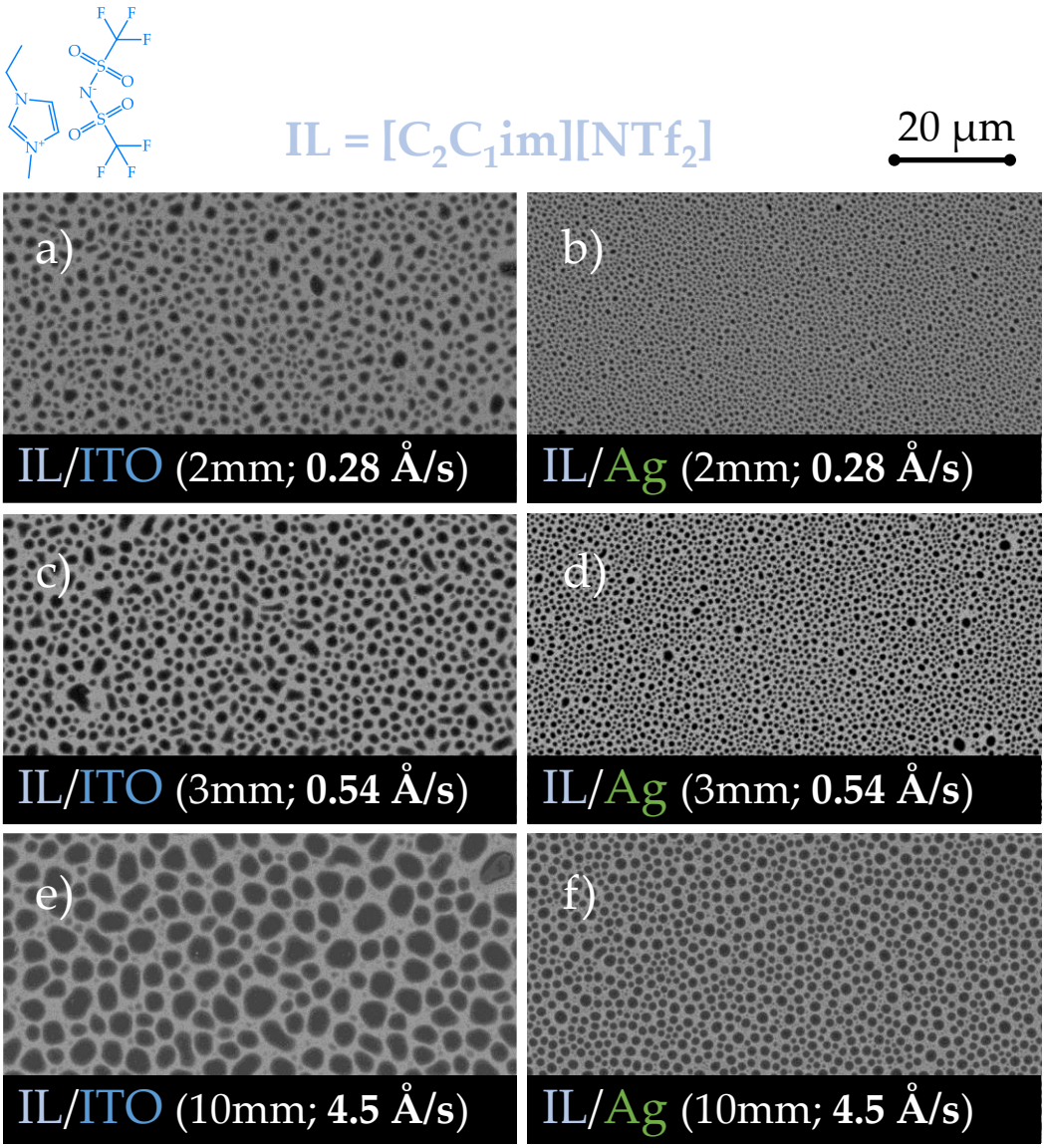

Figure S18. Morphology of micro-/nanodroplets of $[C_2C_1im][NTf_2]$ (40 ML) fabricated by vacuum thermal evaporation onto ITO/glass (a, c, e) and Ag/ITO/glass (b, d, f) using Knudsen effusion cells with different orifice diameters: 2 mm (a, b); 3 mm (c, d); no disk with orifice/evaporation done directly from the cell body (e, f). An evaporation temperature of 503 K was used, and the substrate temperature was kept at 283 K. Surface coverages of 30, 34, 36, 35, 46, and 43 % were derived by image processing of Figures a, b, c, d, e, and f, respectively. SEM micrographs (top views) obtained by backscattered electron imaging.

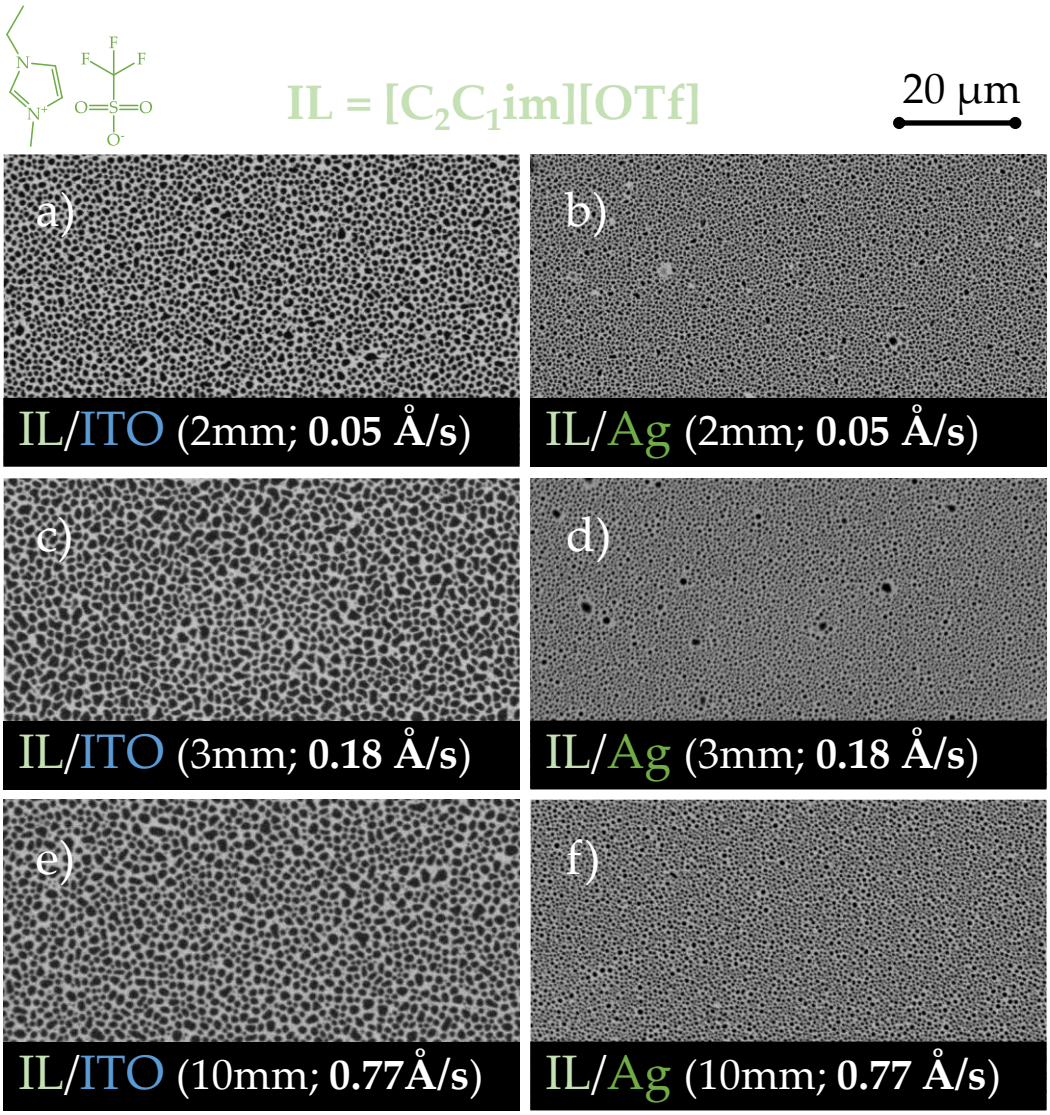

Figure S19. Morphology of micro-/nanodroplets of [C2C1im][OTf] (40 ML) fabricated by vacuum thermal evaporation onto ITO/glass (a, c, e) and Ag/ITO/glass (b, d, f) using Knudsen effusion cells with different orifice diameters: 2 mm (a, b); 3 mm (c, d); no disk with orifice/evaporation done directly from the cell body (e, f). An evaporation temperature of 503 K and 513 K was used, and the substrate temperature was kept at 283 K. Surface coverages of 46, 41, 49, 38, 46, and 39 % were derived by image processing of Figures a, b, c, d, e, and f, respectively. SEM micrographs (top views) obtained by backscattered electron imaging.

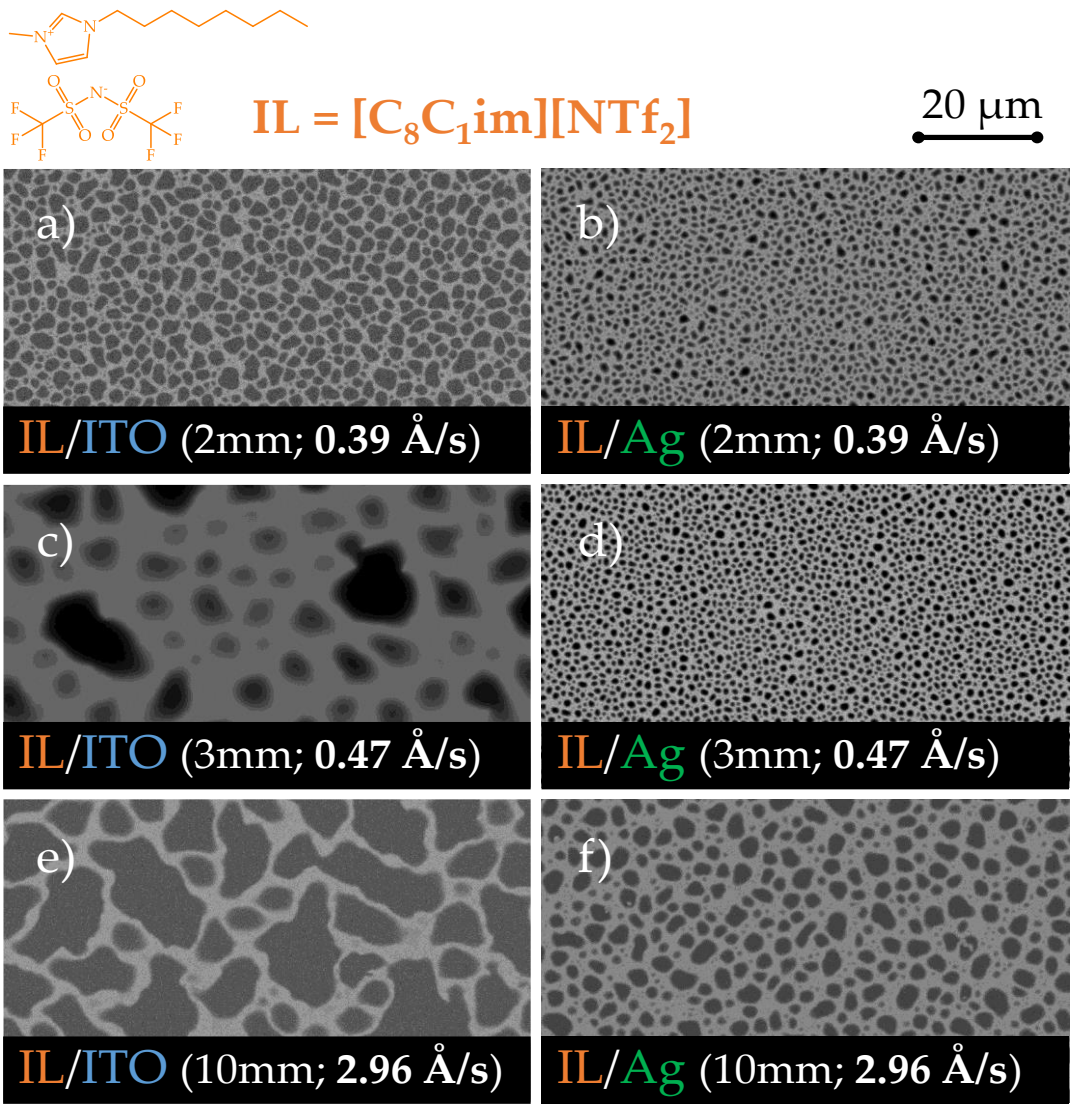

Figure S20. Morphology of micro-/nanodroplets of [C_8C_1im][NTf_2] (40 ML) fabricated by vacuum thermal evaporation onto ITO/glass (a, c, e) and Ag/ITO/glass (b, d, f) using Knudsen effusion cells with different orifice diameters: 2 mm (a, b); 3 mm (c, d); no disk with orifice/evaporation done directly from the cell body (e, f). An evaporation temperature of 503 K was used, and the substrate temperature was kept at 283 K. The image processing was not able to derive with accuracy the surface coverage of the films. SEM micrographs (top views) obtained by backscattered electron imaging.

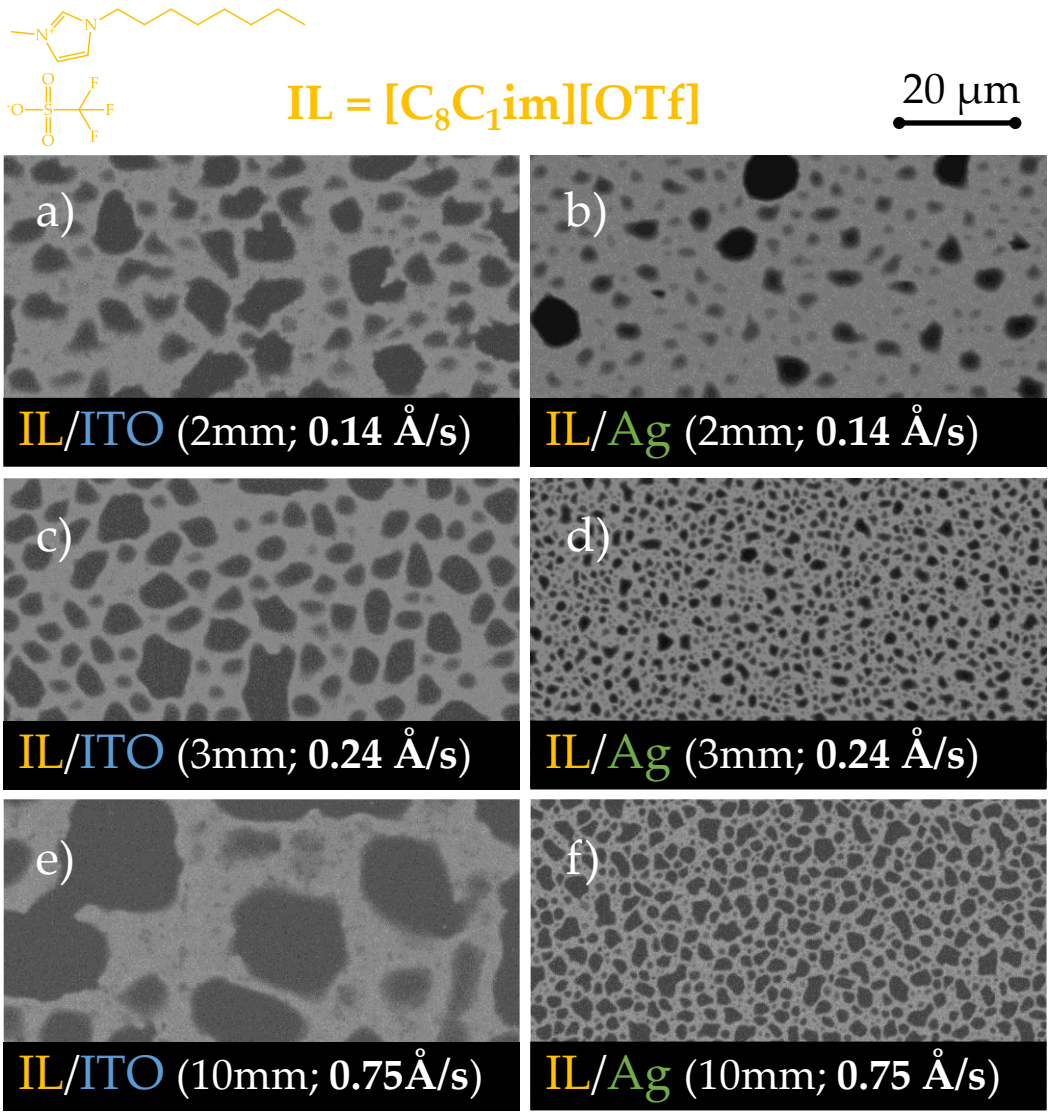

Figure S21. Morphology of micro-/nanodroplets of [C_8C_1im][OTf] (40 ML) fabricated by vacuum thermal evaporation onto ITO/glass (a, c, e) and Ag/ITO/glass (b, d, f) using Knudsen effusion cells with different orifice diameters: 2 mm (a, b); 3 mm (c, d); no disk with orifice/evaporation done directly from the cell body (e, f). An evaporation temperature of 503 K was used, and the substrate temperature was kept at 283 K. The image processing was not able to derive with accuracy the surface coverage of the films. SEM micrographs (top views) obtained by backscattered electron imaging.

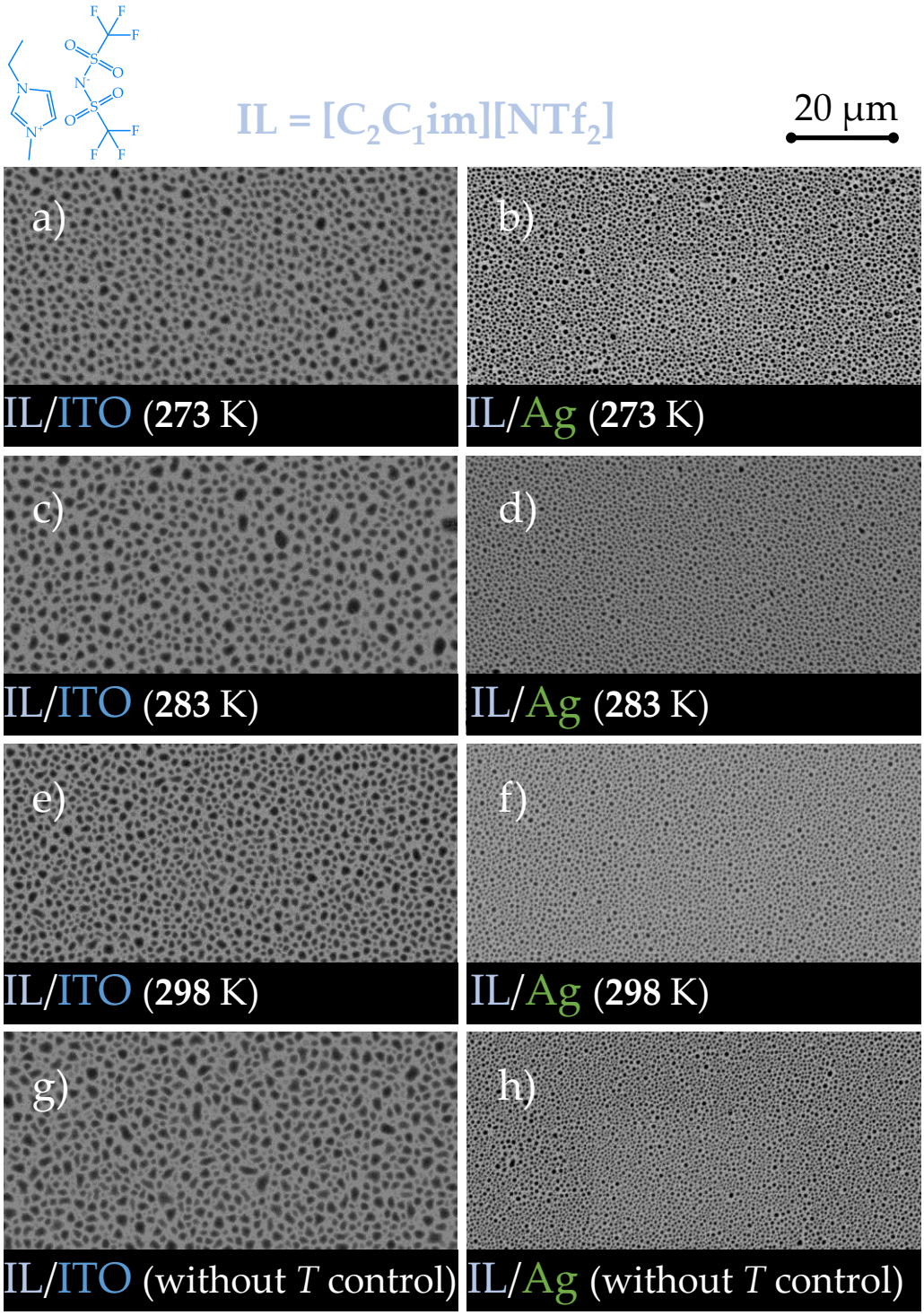

Figure S22. Morphology of micro-/nanodroplets of [C_2C_1im][NTf_2] (40 ML) fabricated by vacuum thermal evaporation (at T = 503 K) onto ITO/glass (a, c, e, g) and Ag/ITO/glass (b, d, f, h) using a Knudsen effusion cell (orifice diameter of 2 mm) and employing different substrate temperatures: 273 K (a, b); 283 K (c, d); 298 K (e, f); without temperature control (g, h). Surface coverages of 30, 34, 30, 34, 34, 32, 32, and 37 % were derived by image processing of Figures a, b, c, d, e, f, g, and h, respectively. SEM micrographs (top views) obtained by backscattered electron imaging.

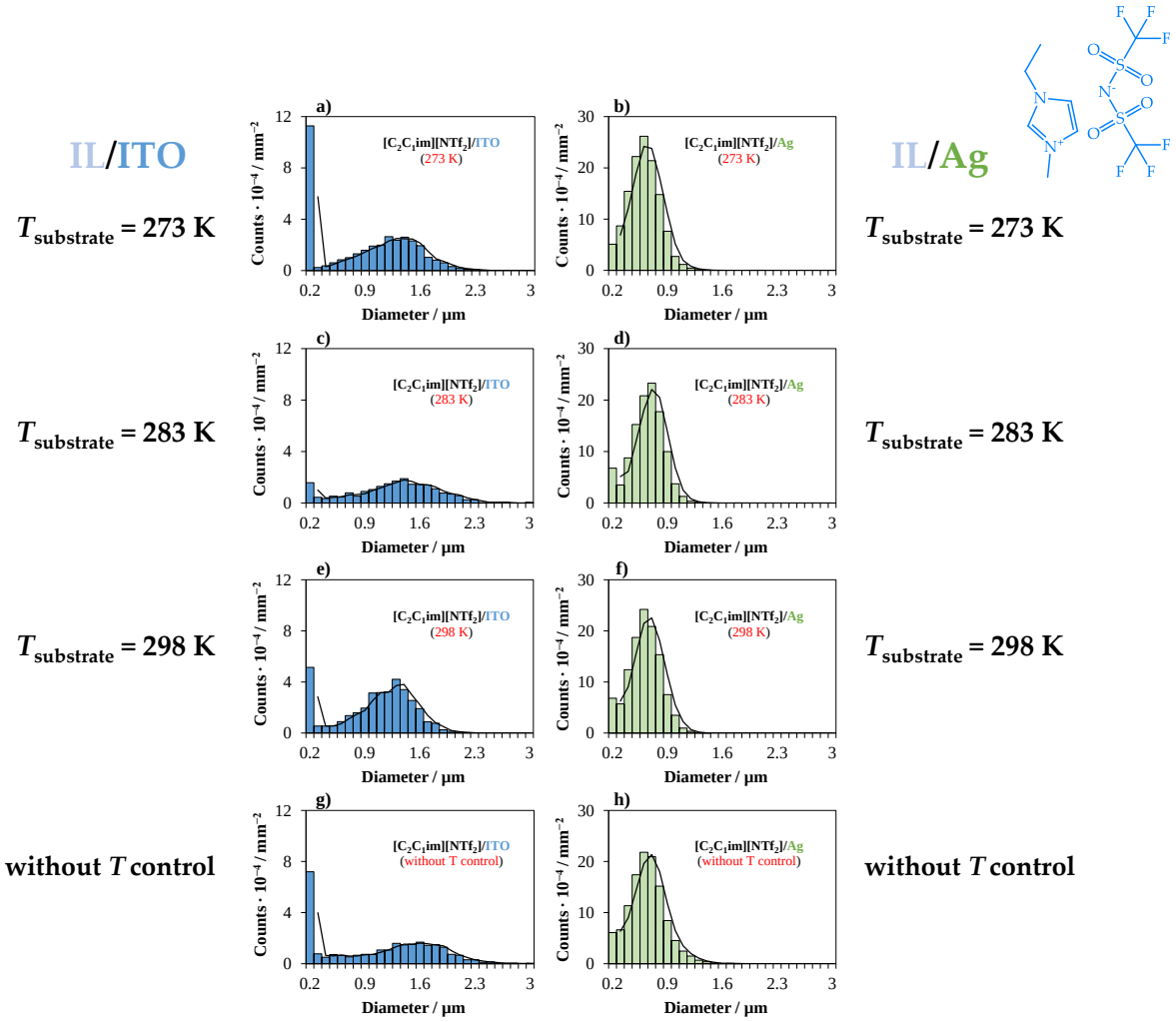

Figure S23. Size distribution of micro-/nanodroplets of [C2C1im][NTf2] (40 ML) fabricated by vacuum thermal evaporation (at T = 503 K) onto ITO/glass (a, c, e, g) and Ag/ITO/glass (b, d, f, g) using a Knudsen effusion cell (orifice diameter of 2 mm) and employing different substrate temperatures: 273 K (a, b); 283 K (c, d); 298 K (e, f); without temperature control (g, h).

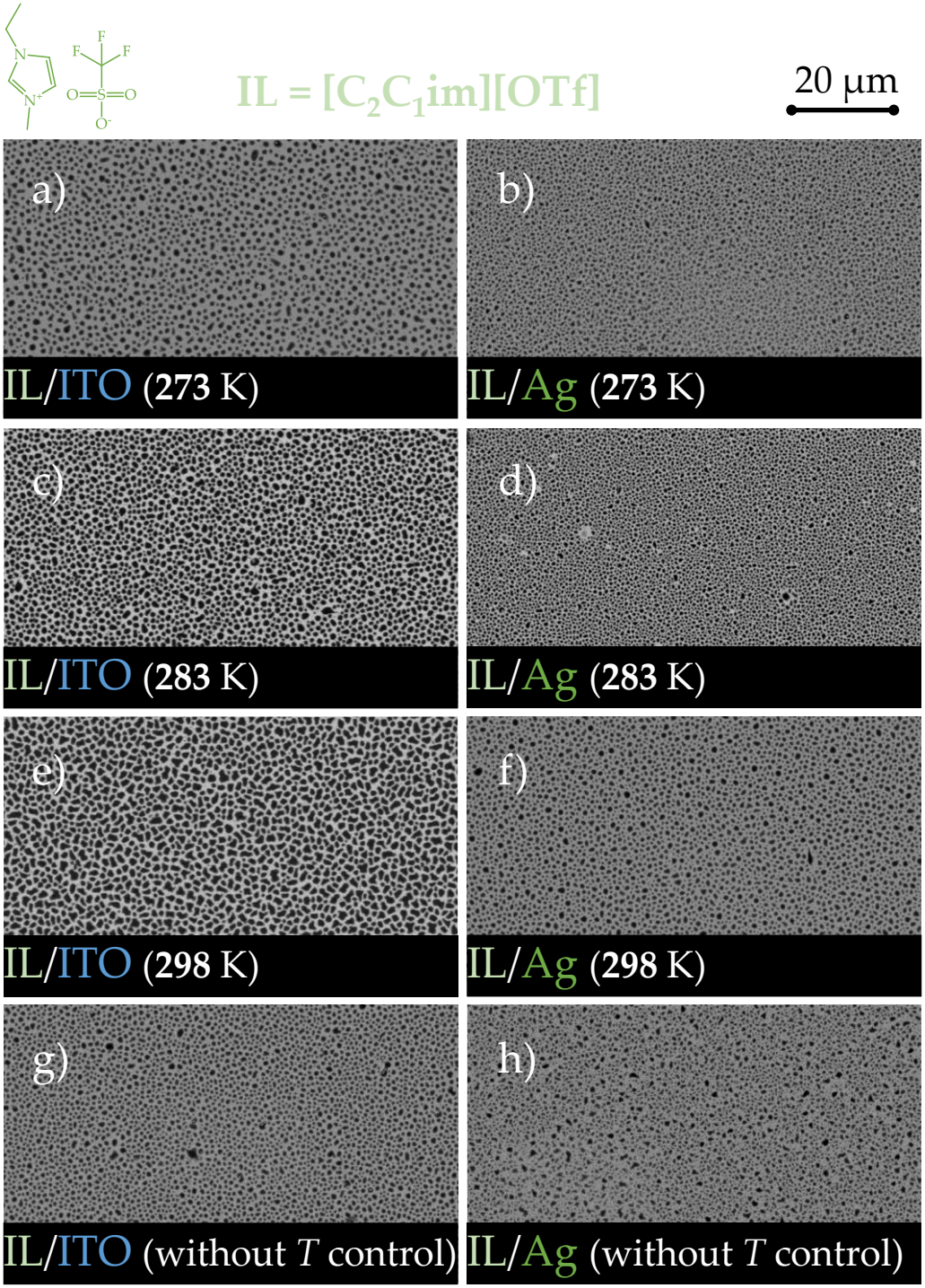

Figure S24. Morphology of micro-/nanodroplets of [C2C1im][OTf] (40 ML) fabricated by vacuum thermal evaporation (at T = 503 K) onto ITO/glass (a, c, e, g) and Ag/ITO/glass (b, d, f, h) using a Knudsen effusion cell (orifice diameter of 2 mm) and employing different substrate temperatures: 273 K (a, b); 283 K (c, d); 298 K (e, f); without temperature control (g, h). Surface coverages of 29, 35, 46, 41, 47, 34, 36, and 34 % were derived by image processing of Figures a, b, c, d, e, f, g, and h, respectively. SEM micrographs (top views) obtained by backscattered electron imaging.

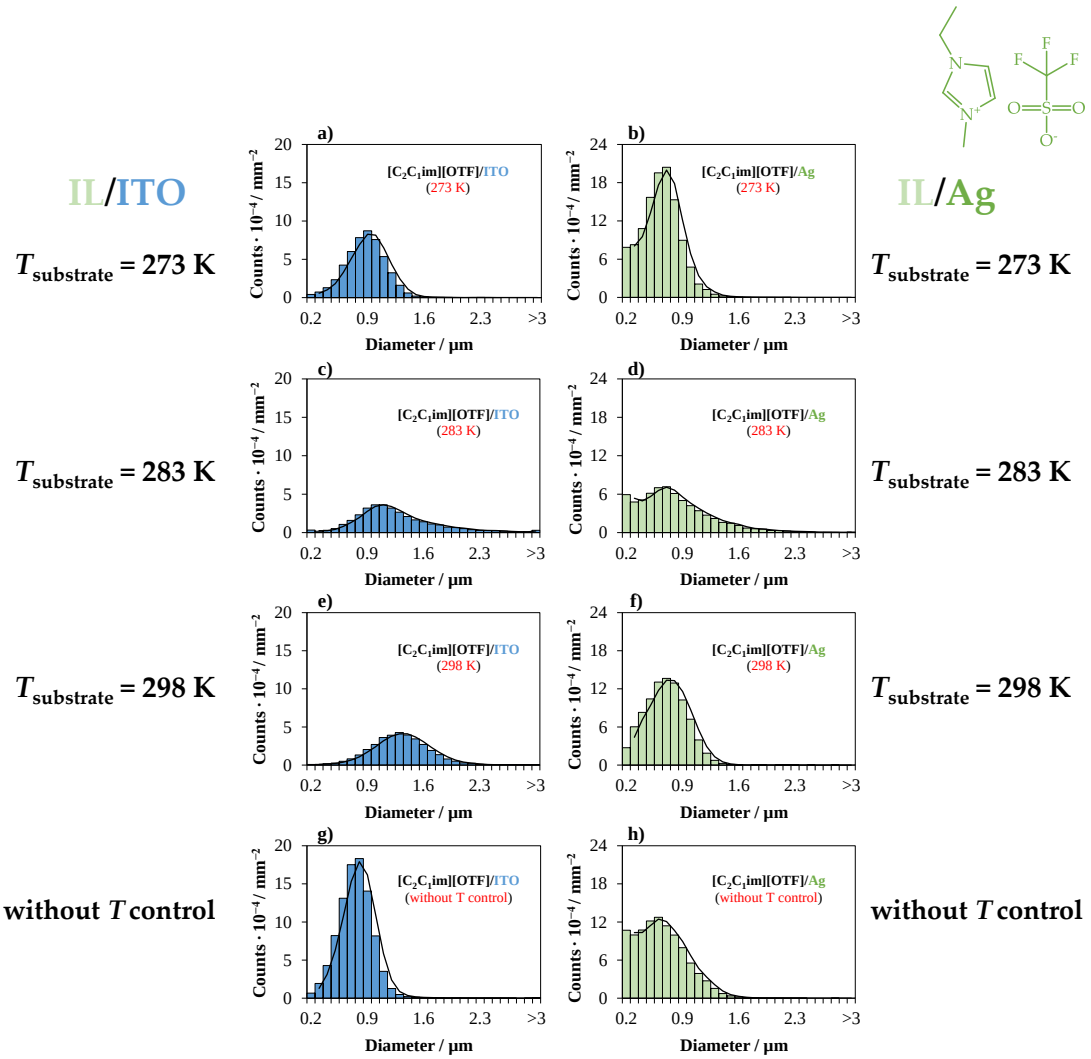

Figure S25. Size distribution of micro-/nanodroplets of [C2C1im][OTf] (40 ML) fabricated by vacuum thermal evaporation (at T = 503 K) onto ITO/glass (a, c, e, g) and Ag/ITO/glass (b, d, f, g) using a Knudsen effusion cell (orifice diameter of 2 mm) and employing different substrate temperatures: 273 K (a, b); 283 K (c, d); 298 K (e, f); without temperature control (g, h).

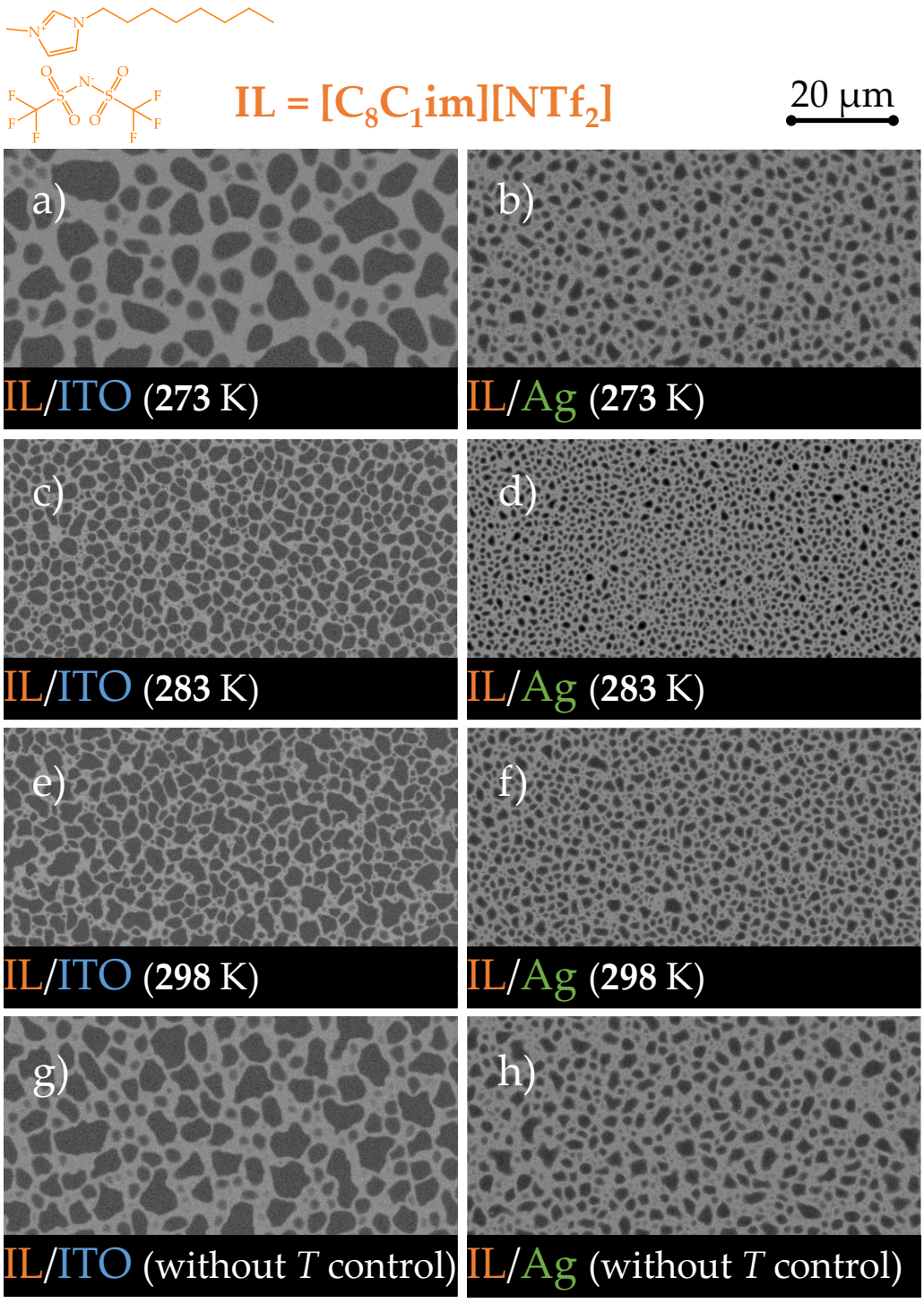

Figure S26. Morphology of micro-/nanodroplets of [C_8C_1im][NTf_2] (40 ML) fabricated by vacuum thermal evaporation (at T = 503 K) onto ITO/glass (a, c, e, g) and Ag/ITO/glass (b, d, f, h) using a Knudsen effusion cell (orifice diameter of 2 mm) and employing different substrate temperatures: 273 K (a, b); 283 K (c, d); 298 K (e, f); without temperature control (g, h). The image processing was not able to derive with accuracy the surface coverage of the films. SEM micrographs (top views) obtained by backscattered electron imaging.

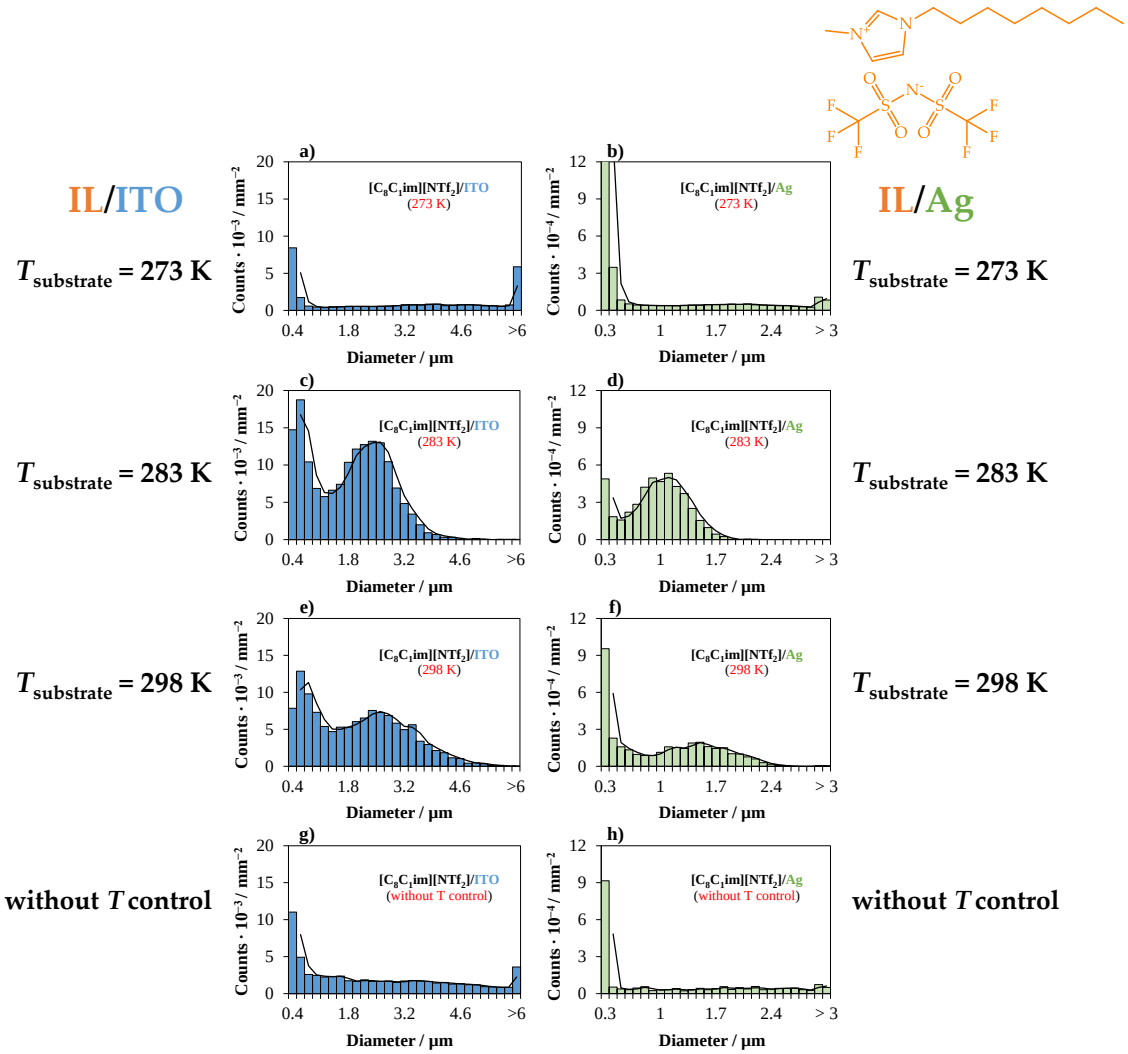

Figure S27. Size distribution of micro-/nanodroplets of [C8C1im][NTf2] (40 ML) fabricated by vacuum thermal evaporation (at T = 503 K) onto ITO/glass (a, c, e, g) and Ag/ITO/glass (b, d, f, g) using a Knudsen effusion cell (orifice diameter of 2 mm) and employing different substrate temperatures: 273 K (a, b); 283 K (c, d); 298 K (e, f); without temperature control (g, h).

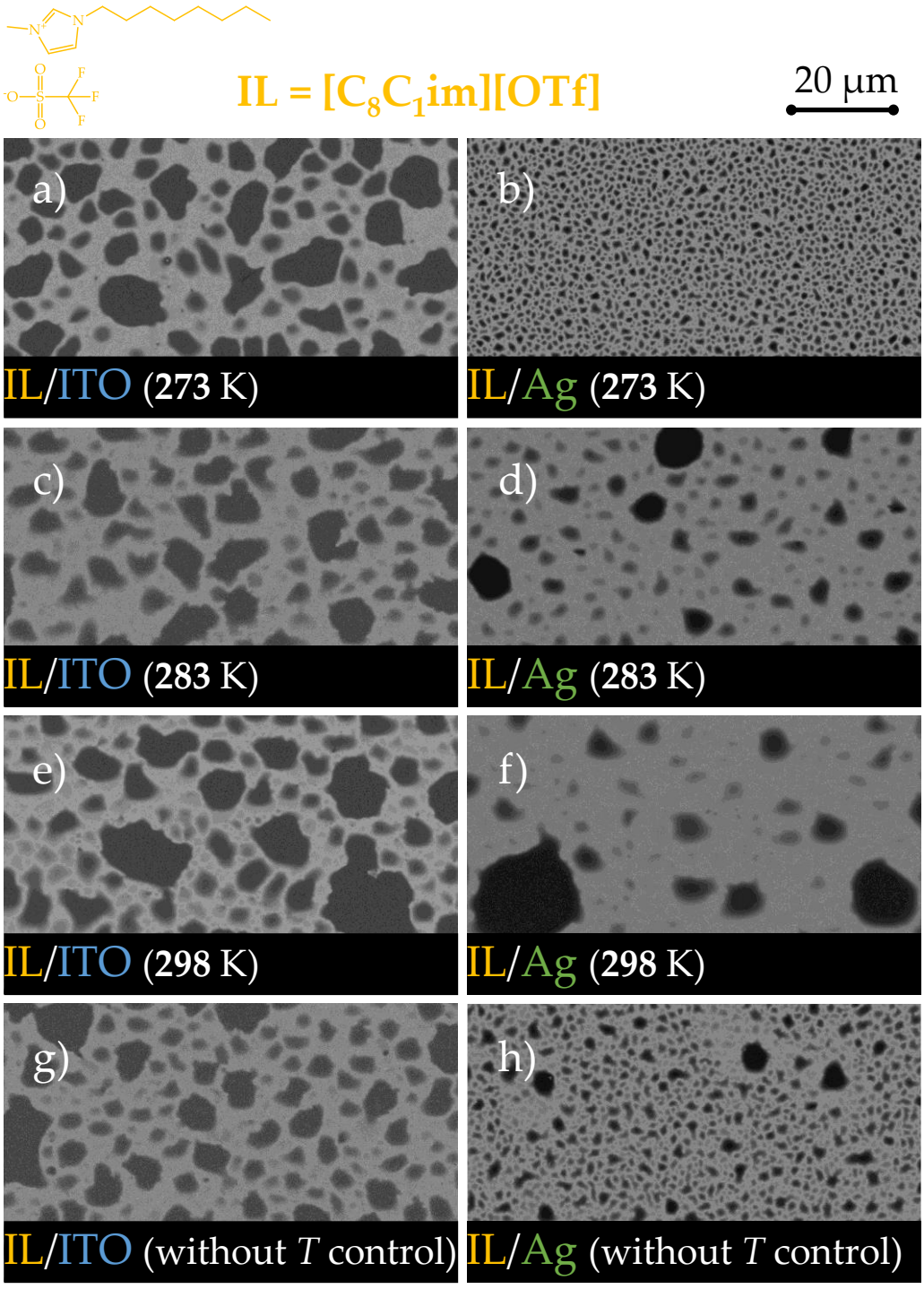

Figure S28. Morphology of micro-/nanodroplets of [C8C1im][OTf] (40 ML) fabricated by vacuum thermal evaporation (at T = 513 K) onto ITO/glass (a, c, e, g) and Ag/ITO/glass (b, d, f, h) using a Knudsen effusion cell (orifice diameter of 2 mm) and employing different substrate temperatures: 273 K (a, b); 283 K (c, d); 298 K (e, f); without temperature control (g, h). The image processing was not able to derive with accuracy the surface coverage of the films. SEM micrographs (top views) obtained by backscattered electron imaging.

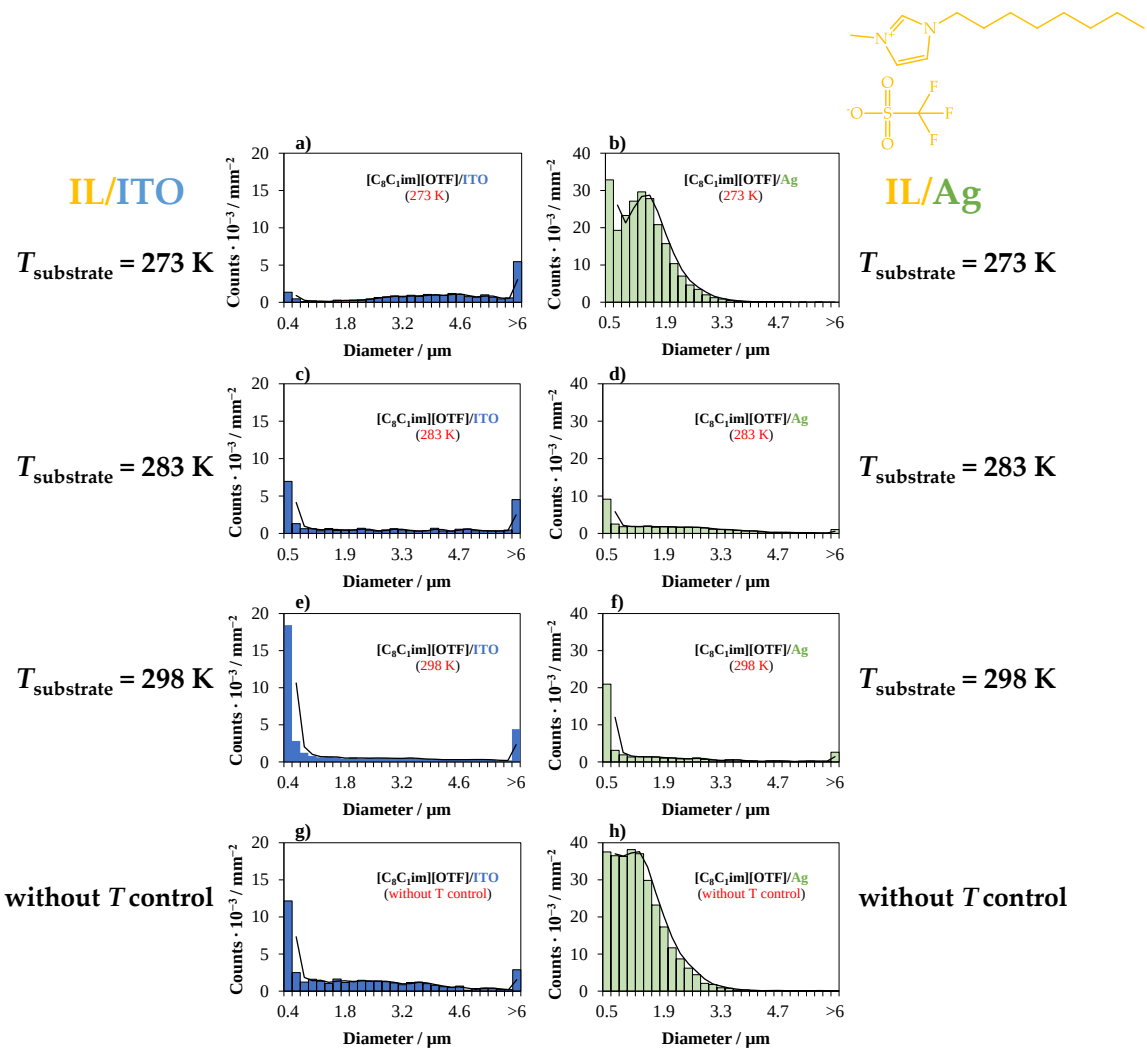

Figure S29. Size distribution of micro-/nanodroplets of [C8C1im][OTf] (40 ML) fabricated by vacuum thermal evaporation (at T = 513 K) onto ITO/glass (a, c, e, g) and Ag/ITO/glass (b, d, f, g) using a Knudsen effusion cell (orifice diameter of 2 mm) and employing different substrate temperatures: 273 K (a, b); 283 K (c, d); 298 K (e, f); without temperature control (g, h).

Table S1. Experimental conditions for the physical vapor deposition/thermal evaporation of each ionic liquid: effusion temperature ($T_{eff.}$); equilibrium vapor pressure (*EVP*); orifice diameter of the Knudsen effusion cell; substrate temperature ($T_{subst.}$); mass flow rate at the substrate surface [Φ (QCM)] and corresponding deposition rate in Å·s^{-1}; deposition time. Experimental variables related to the study of the effect of the mass flow rate on the morphology of different ionic liquids deposited with 40 ML on the ITO/glass and Ag/ITO/glass surfaces.

Precursor	$T_{eff.}$	$T_{subst.}$	EVP	Orifice diameter	Φ (QCM)	Deposition rate	Deposition time
	K	K	Pa	mm	ng·cm^{-2}·s^{-1}	Å·s^{-1}	s
			[C$_n$C$_1$im][NTf$_2$] (40 ML) / substrate | substrates: Ag/ITO/glass; ITO/glass				
	473.2		0.04 [a]	2.1	1.2	0.08 ± 0.01	3750
	503.2		0.25 [a]	2.1	4.3	0.39 ± 0.08	1071
	533.2		1.00 [a]	2.1	11.2	0.74 ± 0.10	395
[C$_2$C$_1$im][NTf$_2$]	473.2	283	0.04 [a]	3.1	1.8	0.12 ± 0.05	2500
	503.2		0.25 [a]	3.1	8.2	0.54 ± 0.05	556
	533.2		1.00 [a]	3.1	22.8	1.50 ± 0.18	200
	503.2			[b]	68.4	4.50 ± 0.52	67
	473.2		0.02 [a]	2.1	1.0	0.08 ± 0.004	4200
	503.2		0.16 [a]	2.1	5.1	0.39 ± 0.04	862
	533.2		0.90 [a]	2.1	14.4	1.10 ± 0.11	305
[C$_8$C$_1$im][NTf$_2$]	473.2	283	0.02 [a]	3.1	1.4	0.11 ± 0.05	3055
	503.2		0.16 [a]	3.1	6.2	0.47 ± 0.06	715
	533.2		0.90 [a]	3.1	19.7	1.50 ± 0.26	224
	503.2			[b]	39.3	2.96 ± 0.25	114
			[C$_n$C$_1$im][OTf] (40 ML) / substrate | substrates: Ag/ITO/glass; ITO/glass				
	473.2			2.1	0.3	0.02 ± 0.02	13600
	503.2			2.1	0.7	0.05 ± 0.04	5440
	533.2			2.1	2.1	0.15 ± 0.06	1813
[C$_2$C$_1$im][OTf]	473.2	283	[c]	3.1	0.8	0.06 ± 0.01	4533
	503.2			3.1	2.5	0.18 ± 0.07	1511
	533.2			3.1	7.1	0.51 ± 0.04	533
	503.2			[b]	10.7	0.77 ± 0.16	353
	473.2			2.1	0.5	0.04 ± 0.02	7800
	513.2			2.1	1.7	0.14 ± 0.02	2229
	533.2			2.1	3.6	0.30 ± 0.05	1040
[C$_8$C$_1$im][OTf]	473.2	283	[c]	3.1	1.1	0.09 ± 0.02	3467
	503.2			3.1	2.9	0.24 ± 0.09	1300
	533.2			3.1	8.8	0.73 ± 0.05	427
	503.2			[b]	9.0	0.75 ± 0.10	416

[a] The EVP at each evaporation temperature was derived from literature data reporting volatility studies of the ILs: [C$_2$C$_1$im][NTf$_2$] and [C$_8$C$_1$im][NTf$_2$], *J. Phys. Chem. B* **2011**, *115*, 10919–10926.

[b] These experiments were performed by removing the disk containing the orifice to maximize the mass flow rate – only the cell body was used.

[c] Accurate data for the EVP of [C$_2$C$_1$im][OTf] and [C$_8$C$_1$im][OTf] were not found elsewhere. Nevertheless, there are reports on the determination of vaporization enthalpies indicating the lower volatility of the [OTF]-based ILs in comparison to their congeners [NTf$_2$]-based ILs. In fact, in this work, at the same evaporation temperature lower deposition rates were observed for [OTf]-based. The EVP of [C$_2$C$_1$im][OTf] and [C$_8$C$_1$im][OTf] at the studied evaporation temperatures are estimated to be within the interval between 0.01 and 1 Pa. In addition, their EVP may be lower than observed for [C$_2$C$_1$im][NTf$_2$] and [C$_8$C$_1$im][NTf$_2$].

Table S2. Experimental conditions for the physical vapor deposition/thermal evaporation of each ionic liquid: effusion temperature ($T_{eff.}$); equilibrium vapor pressure (*EVP*); orifice diameter of the Knudsen effusion cell; substrate temperature ($T_{subst.}$); mass flow rate at the substrate surface [Φ (QCM)] and corresponding deposition rate in Å·s^{-1}; deposition time. Experimental variables related to the study of the effect of the substrate temperature on the morphology of different ionic liquids deposited with 40 ML on the ITO/glass and Ag/ITO/glass surfaces.

Precursor	T_{eff}	$T_{subst.}$	EVP	Orifice diameter	Φ (QCM)	Deposition rate	Deposition time
	K	K	Pa	mm	ng·cm^{-2}·s^{-1}	Å·s^{-1}	s
[C$_n$C$_1$im][NTf$_2$] (40 ML) / substrate | substrates: Ag/ITO/glass; ITO/glass							
[C$_2$C$_1$im][NTf$_2$]	503.2	273	0.25 [a]	2.1	6.7	0.44 ± 0.09	682
		283			4.3	0.39 ± 0.09	769
		298			6.5	0.43 ± 0.08	698
		Without T control [b]			6.5	0.43 ± 0.05	698
[C$_8$C$_1$im][NTf$_2$]	503.2	273	0.16 [a]	2.1	5.9	0.45 ± 0.05	747
		283			5.1	0.39 ± 0.04	862
		298			5.8	0.44 ± 0.08	764
		Without T control [b]			5.4	0.41 ± 0.09	820
[C$_n$C$_1$im][OTf] (40 ML) / substrate | substrates: Ag/ITO/glass; ITO/glass							
[C$_2$C$_1$im][OTf]	503.2	273	[c]	2.1	1.0	0.07 ± 0.03	3886
		283			0.7	0.05 ± 0.04	5440
		298			0.7	0.05 ± 0.02	5440
		Without T control [b]			0.6	0.04 ± 0.03	6800
[C$_8$C$_1$im][OTf]	513.2	273	[c]	2.1	2.2	0.18 ± 0.03	1733
		283			1.7	0.14 ± 0.02	2229
		298			3.0	0.25 ± 0.01	1248
		Without T control [b]			2.4	0.20 ± 0.03	1560

[a] The EVP at each evaporation temperature was derived from literature data reporting volatility studies of the ILs: [C$_2$C$_1$im][NTf$_2$] and [C$_8$C$_1$im][NTf$_2$], *J. Phys. Chem. B* **2011**, *115*, 10919–10926.

[b] These experiments were performed by turning the refrigerated circulating bath responsible to kept $T_{subst.}$ Constant.

[c] Accurate data for the EVP of [C$_2$C$_1$im][OTf] and [C$_8$C$_1$im][OTf] were not found elsewhere. The EVP of [C$_2$C$_1$im][OTf] and [C$_8$C$_1$im][OTf] at the studied evaporation temperatures are estimated to be within the interval between 0.01 and 1 Pa. In addition, their EVP may be lower than observed for [C$_2$C$_1$im][NTf$_2$] and [C$_8$C$_1$im][NTf$_2$].